DEVELOPMENT OF A CAVITATION EROSION RESISTANT ADVANCED MATERIAL SYSTEM

By

Kendrick H. Light

B.S. University of Maine, 1993

A THESIS

Submitted in Partial Fulfillment of the

Requirements for the Degree of

Master of Science

(in Mechanical Engineering)

The Graduate School

The University of Maine

August, 2005

Advisory Committee:

Vincent Caccese, Associate Professor of Mechanical Engineering, Advisor

Donald A. Grant, R.C. Hill Professor and Chairman of Mechanical Engineering

Senthil S. Vel, Assistant Professor of Mechanical Engineering

Library Rights Statement

In presenting this thesis in partial fulfillment of the requirements for an advanced degree at The University of Maine, I agree that the Library shall make it freely available for inspection. I further agree that permission for "fair use" copying of this thesis for scholarly pruposes may be granted by the Librarian. It is understood that any copying or publication of this thesis for financial gain shall not be allowed without my written permission.

Signature:

Date:

DEVELOPMENT OF A CAVITATION EROSION RESISTANT ADVANCED MATERIAL SYSTEM

By Kendrick H. Light

Thesis Advisor: Dr. Vincent Caccese

An Abstract of the Thesis Presented
in Partial Fulfillment of the Requirements for the
Degree of Master of Science
(in Mechanical Engineering)

August, 2005

Advancements in both the design and construction of high-speed naval vessels have necessitated the evaluation of the building materials in a cavitating environment. Given their weight advantages, construction materials are often either aluminum or glass reinforced polymer (GRP) composites. Historically, neither of these materials has performed well in a cavitating environment. The objective of this effort was to evaluate cavitation erosion protection alternatives for a GRP composite structure used in a cavitating environment. Screening of the various design alternatives was done using the ASTM G32 vibratory induced cavitation test method and a relative ranking of each protection system was generated. Results from the testing show that a GRP composite system can be designed to greatly increase the cavitation erosion resistance of the material, but this resistance remains below common metallic materials. A solution identified during this study involves the use of durable elastomer materials as the protection mechanism.

Acknowledgements

The author gratefully acknowledges funding for this project through the University of Maine from the Office of Naval Research under grant number N00014-01-1-0916. Dr. Roshdy S. Barsoum of ONR is the cognizant program officer. His support and encouragement is greatly appreciated. The author would also like to thank Milt Crichfield, Loc Nguyen and Gene Camponeschi of NSWC Carderock (NSWCCD) for their assistance and advice. Furthermore, the support of the other partners involved in this effort, particularly, Steven Loui, Todd Pelzer and Eric Schiff of Pacific Marine, Navatek Division and the project team at the University of Maine including Vince Caccese, Randy Bragg and Keith Berube. The guidance and support of other personnel at Applied Thermal Sciences is also acknowledged including Larry Thompson, Steve Webber and Josh Walls. Other ATS personnel include Eric Shorey who assisted greatly in the testing phase of this effort and Martha Mundy for her diligent assistance with the background research. Acknowledgements also go out to Ronnie Oliver and Julie Brown as engineering interns for their help during the arduous testing process. Lastly, I would like to acknowledge the help and support of Vince Caccese in the preparation and editing of this report. His unwavering support of this thesis work has provided the ultimate catalyst for the success of this effort.

Table of Contents

ACKNOWLEDGEMENTS ii

LIST OF TABLES vi

LIST OF FIGURES vii

Chapter

1. INTRODUCTION 1

    1.1 Objectives 5

    1.2 Scope of Work 6

2. BACKGROUND RESEARCH 7

    2.1 Cavitation Erosion Phenomenon 7

    2.2 Material Property Correlation 9

    2.3 Metals and Coatings 10

    2.4 Rain Erosion Studies 10

    2.5 Previous Composite Material Testing for Cavitation Erosion 13

3. EROSION RESISTANT MATERIAL SYSTEM CONSIDERATIONS 16

    3.1 Composite Erosion Protection System 18

        3.1.1 Fiber Properties 18

        3.1.2 Resins 19

        3.1.3 Sandwich Core Materials 20

3.1.4 Laminate Geometry 21
3.2 Surface Protection Layers 23
3.3 Metal Skins 24
4. CAVITATION TESTING 25
4.1 Test Apparatus 26
4.2 Test Method 27
4.3 Reduction of Test Results 29
4.4 Calibration of Test Setup and Procedures 31
4.5 Repeatability of Modified Test Using Aluminum Samples 34
4.6 Addition of Data Acquisition System for Overnight Testing 35
5. DISCUSSION OF TEST RESULTS 36
5.1 Metals 36
5.2 Composites 41
5.3 Elastomers 44
5.3.1 Ethylene Propylene Diene Monomer (EPDM) based Elastomers 45
5.3.2 Fluorinated Elastomers 48
5.3.3 Polyurethane based Elastomers 50
5.3.4 Silicone based Elastomers 53
5.3.5 Polychloroprene based Elastomer 54
5.4 Other 55
6. SUMMARY AND RECOMMENDATIONS 57
REFERENCES 61

APPENDIX – SUMMARY OF TEST RESULTS 63

BIOGRAPHY OF THE AUTHOR 66

List of Tables

Table 3.1 - Fiber property comparison 19

Table 3.2 - Resin property comparison 20

Table 3.3 - Core material property comparison (properties courtesy of Baltek Corporation) 21

Table 3.4 - Manufactured laminate geometries 22

Table 4.1 – Comparison of normalized MDE for Ni 200 Standard versus Modified Procedure 33

Table 5.1 - List of custom formulated Pelseal® Technologies samples tested 49

Table A.1 – Summary of complete test results 63

Table A.2 – Sample test data sheet 65

List of Figures

Figure 1.1 - Photographs of cavitation generated by high speed lifting body shapes. [University of Tokyo] 2

Figure 2.1 – Schematic of asymmetrical bubble collapse showing liquid jet impingement [Morch, 1979] 8

Figure 2.2 - Photograph of actual collapsing cavitation bubble. [Center for Industrial and Medical Ultrasound, University of Washington] 9

Figure 3.1 – Schematic representation of different types of material systems 17

Figure 3.2 – Qualitative assessment of marine composite construction materials [Greene,1999] 17

Figure 3.3 - Laminate weave geometries [Strong, 1989] 22

Figure 4.1 – Photograph of the experimental test apparatus 26

Figure 4.2 – Close-up photograph of the specimen holder 26

Figure 4.3 - Example Cumulative Erosion-Time Curve 30

Figure 4.4 - MDE for Ni 200 from independent lab tests using ASTM procedures 31

Figure 4.5 – Erosion rate of Ni 200 samples Using Modified Procedures 32

Figure 4.6 – Repeatability of 6061-T6 Aluminum Samples 34

Figure 5.1 – Plot of MDE versus time for all Aluminum 6061-T6 samples 38

Figure 5.2 – Photograph of aluminum 6061-T6 sample #096 after testing 38

Figure 5.3 – Plot of MDE versus time for 316L stainless steel samples 39

Figure 5.4 – Cavitation damage of a 316L stainless steel sample #040 40

Figure 5.5 – Summary results of cavitation resistance of candidate metal samples 40

Figure 5.6 – Test sample of E-glass/8084 (left) and Carbon/8084 (right) showing matrix and fiber erosion 43
Figure 5.7 – Summary results of cavitation resistance of composite samples 43
Figure 5.8 – Carbon fiber over PVC core samples showing core damage 44
Figure 5.9 – Quartz fiber over PVC core sample showing core damage. 44
Figure 5.10 – Sheet EPDM results 47
Figure 5.11 – EPDM rubber samples, sheet (left) and liquid (right) 48
Figure 5.12 – PLV 2100 sample showing typical damage pattern 50
Figure 5.13 - Herculiner® sample #051 showing erosion damage 51
Figure 5.14 – Rhino Linings sample #110 showing typical damage including bubble formation under the horn tip 52
Figure 5.15 – Biocoat-A screening sample #119 after 2,936 minutes of test time. No visible cracking or pitting 54
Figure 5.16 – Cuproprene sample showing damage to embedded copper-nickel granules 55
Figure 5.17 – Tested samples of CeRam-Kote 54 on aluminum substrates showing cavitation damage 56

1. Introduction

The U.S. Navy is currently pursuing the development of advanced hull forms to meet future naval requirements. One capability that is universally being sought from these new hull forms is the ability to operate above fifty knots for sustained periods. In this environment, naval designers will need to make special considerations for any hull structure that remains below the waterline. At these speeds changes in hull curvature can drop the flowing water below its vapor pressure and induce cavitation. In a relatively short amount of time, the material at the cavitating hull section may begin to show signs of damage from having to absorb the energy of the impinging, collapsing bubbles. This can quickly lead to significant material loss by erosion of the weakened and damaged material. If left unchecked, both hydrodynamic performance and structural degradation can result.

There is a current need to evaluate the cavitation erosion resistance of materials and protective systems for advanced ship hull sections. Examples of the cavitation generated by moving bodies due to geometric shape changes are illustrated in Figure 1.1. The damage and material loss caused by cavitation erosion of naval surface vessels has traditionally only been seen in the areas of the propeller and rudder components. These components are typically constructed from relatively cavitation resistant materials such as stainless steel or NiAl (Nickel Aluminum) bronze. Both of these materials have a long history of being used in cavitating environments and are repairable when damage does occur. The downfall of these materials however is their excessive weight when evaluating these materials for the construction of a complete high-speed hull form. Most

of the advanced hull forms being proposed to the U.S. Navy make use of much lighter materials such as aluminum or glass reinforced polymer (GRP). Both of these materials, however, are documented as being very poor with respect to their cavitation erosion resistance.

Figure 1.1 - Photographs of cavitation generated by high speed lifting body shapes. [University of Tokyo]

The work presented herein was performed under the Modular Advanced Composite Hull-form (MACH) project where the focus is to develop and test hybrid metal/composite structural systems for naval ship applications. The MACH project is part of a joint effort between the University of Maine, the Navatek division of Pacific Marine (PACMAR) of Honolulu, HI, and Applied Thermal Sciences (ATS) of Sanford, Maine and is performed in conjunction with the Navy Surface Warfare Center at Carderock, MD (NSWCCD). The mission of the MACH program is to develop fast efficient surface vessels that use additional underwater bodies attached to a more traditional hull-form. The primary motivation for this project is to provide alternatives to conventional hull construction techniques and conventional hull forms by using modular hybrid construction methods.

One goal of the MACH project is to develop a methodology of designing and constructing lightweight hybrid composite/metallic hull forms to be used on high-speed ships. The goal is to deploy ships where more payload and/or higher speeds can be achieved at little or no additional power consumption and with excellent sea keeping ability.

Figure 1.2 shows one example vessel called the MIDFOIL developed by Navatek where a hydrofoil and a parabolic lifting body shape are combined with a catamaran hull to achieve additional buoyancy and dynamic lift which greatly improves the performance and sea-keeping of the vessel. Relatively inexpensive pilot tests on the MIDFOIL and similar vessels have shown that this method has great advantage for fast military support craft and commercial vessels such as ferries. Recent studies have shown that the addition of underwater bodies can dramatically improve speed, reduce fuel consumption and increase payload. These efforts have also demonstrated that composite material construction can bring about increased structural efficiency.

The method proposed for construction of a composite/metal hybrid version of the underwater lifting body is to use a skin made of composite materials attached to a metal framework. Figure 1.3 shows a schematic of this concept. This type of system will allow for ease of maintenance of equipment housed inside the lifting body and it will provide a metal skeleton to facilitate attachment of propulsion equipment. The skin design is of monocoque, stiffened or sandwich construction depending upon structural requirements. It is subsequently attached to the metal structure using a hybrid connection. Detailing this connection to have adequate strength and watertight integrity is imperative.

Figure 1.2 - Midfoil Craft with Underwater Lifting Body

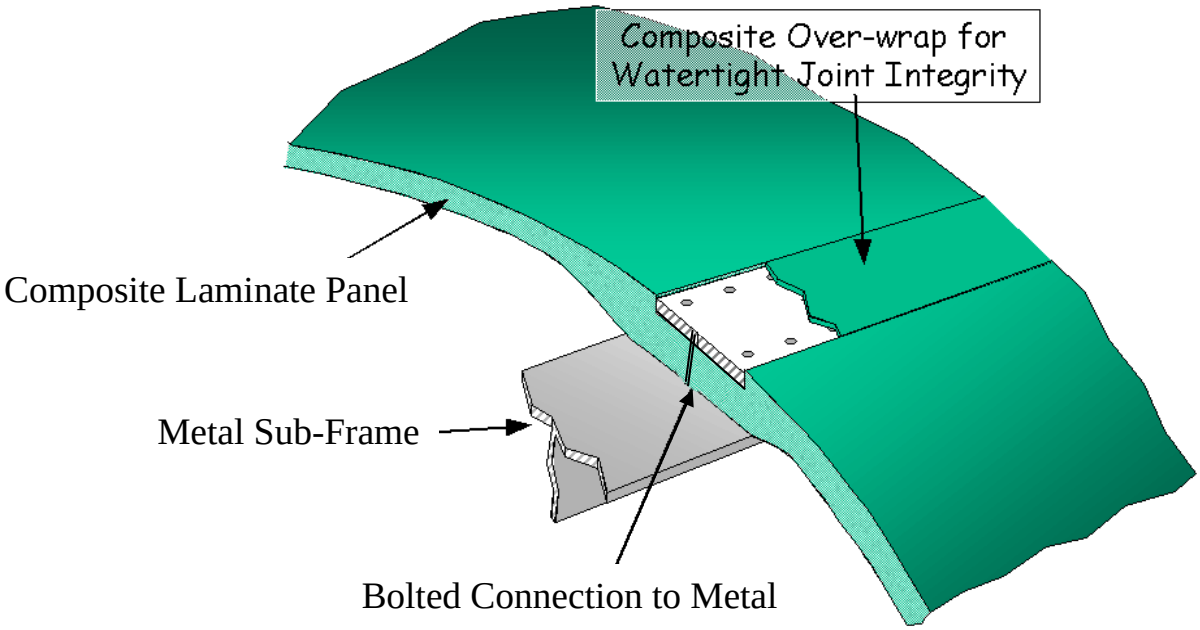

Figure 1.3 - Hybrid Structure Constructed Using GRP Composite Skin Over Metal Substructure

The MACH program hopes to provide a cost effective methodology of helping ship manufacturers achieve the goals of lightweight, high speed vessels that meet future U.S. Navy requirements. Cavitation is anticipated on these lifting bodies due to the high-speed design of these ships. Depending on the specific design of the lifting body, ship designers expect cavitation inception in the range of 45-50 knots. Cavitation is likely to initiate at localized regions such as where the vertical struts attach or other sharp changes in geometry. As speed is increased above the inception limit, cavitation will intensify in these localized regions and then begin to form along the upper surface of the lifting body as depicted in Figure 1.1. The image on the left shows what is commonly referred to as sheet cavitation along the upper surface. The image on the right shows both the sheet cavitation as well as cloud cavitation on the right side of the image. Both of these cavitation modes are expected on the lifting bodies as ship speeds are increased. Given this design methodology and the anticipated cavitating environment, research is needed on how to make composite materials resistant to the damaging effects of cavitation or how to provide a protective envelope in the regions prone to cavitation. In order to insure the utility of GRP components in these severe operating conditions, the MACH program initiated a research task to identify methods of making GRP panels more resistant to the effects of cavitation erosion. The research presented herein is the results of that task.

1.1 Objectives

An engineering study was conducted to identify methods that increase the cavitation erosion resistance of hybrid composite/metal structures. A number of advanced material system concepts were investigated as follows:

1) Advanced durable composite shell,
2) Composite shell with cladded metal or ceramic coatings, and
3) Composite shell overlaid with a metallic outer skin

Included in the objectives of this effort is the ability to adapt the cavitation erosion resistant material system to a full-scale ship manufacturing process. A proof-of-concept study was embarked upon that quantifies the relative cavitation erosion resistance of numerous material systems using a modified ASTM G32 test method.

1.2 Scope of Work

The focus of this research effort is the development of one or more methods for making GRP panels more resistant to the effects of cavitation erosion. Section 2 describes the pertinent theory behind cavitation and its effects on structural materials and includes a literature review of previous testing with composite materials. Candidate material system designs are discussed in Section 3 along with the advantages of each. Section 4 discusses the test method used to rank the material systems as well as the specific materials tested. The results of the cavitation testing are presented in detail in Section 5. A final summary, conclusion and recommendation is given in Section 6 for the design and construction of a cavitation erosion resistant material system for use with GRP panel hull structures.

2. Background Research

2.1 Cavitation Erosion Phenomenon

Understanding the basic phenomena associated with cavitation erosion and researching previous work done with composite materials in these types of environments is essential to the development of a viable cavitation erosion protection system. Historically, composite materials have been poor in their resistance to cavitation attack due to the erosion of the matrix material. It has been noted in the literature that the greatest amount of work done on the erosion resistance of composite materials comes from rain erosion tests in the aerospace industry [Hammond et al., 1993]. There are some parallels to be drawn between these two environments and it has been cited that the methods used to improve the performance are the same [Hammond et al., 1993].

In order to understand a material's response to cavitation attack, it is necessary to first understand the basic mechanisms of cavitation. The term cavitation refers to the phenomena of the formation and collapse of gas/vapor bubbles within a liquid. When the pressure in a fluid drops below the vapor pressure, a bubble is formed. Once the liquid pressure recovers, the bubble collapses. The actual dynamics of the bubble collapse has been extensively reported by numerous researchers [Morch, 1979] and will only be summarized herein. The environment in which the bubble is formed has an important effect on the resulting collapse dynamics. A single bubble formed far from any boundary will collapse spherically. The region of highest pressure in this instance is the geometric center of the bubble where a spherical shock wave is emitted. Under most realistic conditions, the presence of a wall or other bubbles in the flow causes a deviation from a

perfectly symmetrical collapse. This asymmetry greatly complicates the bubble collapse dynamics and results in the formation of a liquid jet by the collapsing bubble surface. This jet is illustrated in Figure 2.1 and shown in-situ in Figure 2.2. If the bubble is near a solid boundary, then this liquid jet acts as a "water hammer" against the surface. Combined with the typical shock wave during collapse, both of these mechanisms can result in damage to the structure. Most researchers, however, credit the liquid jet as being the major damage mechanism. In addition to the effect of a single bubble collapse, the idea of magnification in impingement pressure due to the cumulative collapse of a cloud of bubbles has been reported as providing as much as a ten fold increase in pressure. Pressures on the order of 900 MPa have been reported at the surface near a cavitation cloud [Morch, 1979]. The effect of this phenomenon on ductile materials is a local strain hardening at the site and an eventual fatigue failure of the material [Veerabhadra Rao et al., 1981]. Further exposure beyond this incubation period leads to cracking and loss of material.

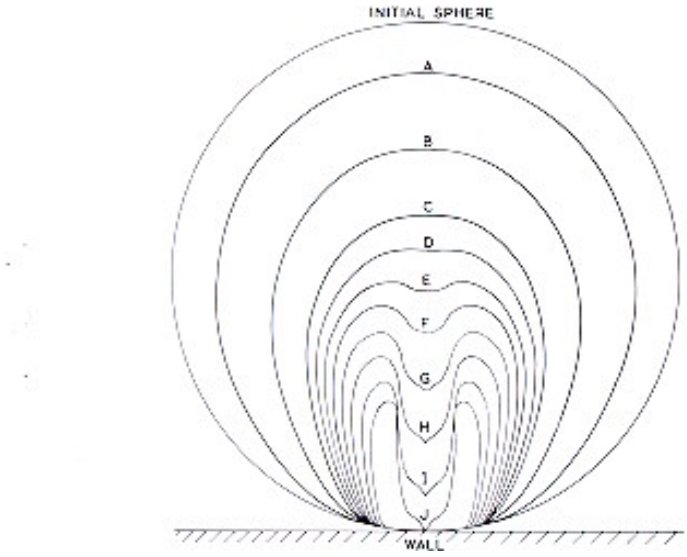

Figure 2.1 – Schematic of asymmetrical bubble collapse showing liquid jet impingement [Morch, 1979]

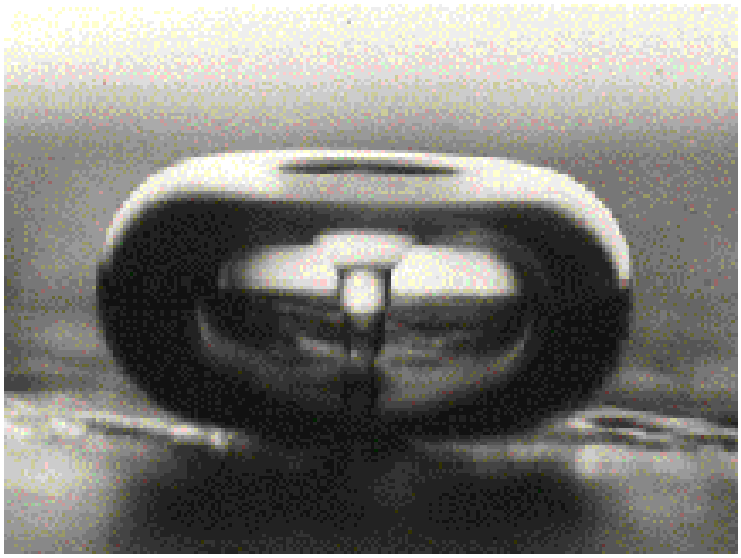

Figure 2.2 - Photograph of actual collapsing cavitation bubble. [Center for Industrial and Medical Ultrasound, University of Washington]

2.2 Material Property Correlation

There have been numerous efforts to correlate a material's resistance to cavitation erosion with some physical material property such as strength, toughness, hardness, etc. Early statistical research pointed to a material's hardness as the primary correlation factor [Heymann, 1970]. This conclusion was recently reiterated by Hattori [Hattori et al., 2003]. Competing theories involve other mechanical properties including a combination of ultimate tensile strength and elastic modulus termed ultimate resilience [Garcia et al., 1967], the combination of ultimate resilience and hardness [Veerabhadra Rao et al., 1981], energy absorption characteristics [Thiruvengadam et al., 1966], and fatigue strength [Richman et al., 1990]. Most of these studies, however, have only considered metallic materials or combinations of metals with hard ceramic coatings. More recent research is trying to factor in the intensity of the cavitation environment [Escaler et al., 2001], [Soyama et al., 2001], [Lecoffre, 1995]. The unique properties of GRP or

elastomer materials, however, are not sufficiently covered in any of the traditional research on cavitation resistance.

2.3 Metals and Coatings

By far the most common material used in cavitating environments is some form of a non-corrosive metal. The family of stainless steels is found in a wide variety of components ranging from pipe and valve components to high speed pump impellers and even blades of large hydroelectric turbines. More specialized materials such as NiAl bronze find application in Naval ship components such as propellers and rudders. Higher performance components that are conscientious about both weight and strength such has hydrofoils are commonly constructed of titanium. Though markedly different in their mechanical properties, these materials all show a high level of cavitation erosion resistance. Other non-corrosive materials such as aluminum are rarely used in these environments because of their poor resistance to erosion. A complete review of all the different grades of materials and formulations used in cavitation environments is beyond the scope of this research. Instead, the vast database of metals research was used to help characterize and understand the damage mechanisms of cavitation. Also, given its widespread use, 316L stainless steel was chosen as the benchmark material in order to compare any future material system.

2.4 Rain Erosion Studies

The work of Hammond [Hammond et al., 1993] and co-workers suggest that one of the biggest databases available for the erosion resistance of composite materials exists from

rain erosion testing in the aerospace industry. Composite aircraft components such as leading edges of wings, flaps and rotors of helicopters all are susceptible to damage from high-speed droplet impingement caused by rain and dense moisture environments. Similarly, the nose regions of missiles, bombs and reentry vehicles must also be designed to withstand high-speed flight through a rain environment.

The mechanism of erosion in a droplet impingement environment like rain has many similarities to that of cavitation. The asymmetrical collapse of a cavitation bubble and the formation of the water jet are analogous to the high-speed impact of small droplets. One study notes that the deformed surfaces of materials subject to both processes are very similar and that the methods used to improve the material's performance were found to be the same [Preece, 1979]. Because of the large database of information and the similar damage mechanisms, a search of the available literature was undertaken in order to find out what material systems are in use for the effective resistance of composite materials to rain erosion.

Early research into the survivability of metals and plastic materials for high-speed aerodynamic structures demonstrated the severity of the environment [Williams, 1952]. Using a rotating arm and a vertical nozzle spray, conditions up to 700 mph could be simulated and different material specimens were evaluated. After testing many different metals, plastics and coated plastics, the results pointed to neoprene rubber as the leading erosion resistant candidate. By the 1970's, the use of composite materials as we know them today was becoming much more prevalent on aircraft and aerodynamic structures.

A study released in July, 1974 by the Hughes Aircraft Company examined different construction techniques for increased rain erosion resistance [Kimmel, 1974]. Utilizing a "whirling" or rotating arm device, the specimens were subjected to impingement by 1.2 mm water droplets at a speed of 333 m/s. The variables evaluated included fiber angle, impact angle, matrix, reinforcement and reinforcement configuration. Measuring the mass loss of each specimen tabulated the results. These results showed that more flexible matrices outperformed rigid formulations. The effect of impact angle with respect to fiber angle showed that the best reinforcement configuration was unidirectional fibers oriented end on with the droplet impact direction. In second place was multidirectional reinforcement with the more traditional 2D fabric constructions showing the least erosion resistance. With respect to the reinforcements, a Nomex/glass composite was found to be far superior to the Kevlar composites tested. These test results are noted as being typical with the results of other previous testing of composite material systems of this time [Kimmel, 1974].

Given the advances in reinforcement materials and matrix formulations, it was desired to find a more recent survey of typical rain erosion protection materials in use today. Kaman Aerospace Corporation conducted one such survey in 1996 [Weigel, 1996]. The objective of this study was to identify a nonmetallic sand and rain erosion resistant material for use on U.S. Army rotorcraft blades. Given the composite substrate and the severity of the environment and operating conditions, this study provides a good basis for assessing today's state of the art in rain erosion protective materials. The investigation primarily focused on elastomeric materials given their superior sand erosion resistance

properties compared to metals [Falcone et al., 1974]. However, it is also reported that elastomeric materials traditionally under perform metals with respect to rain erosion resistance. The study included moldable and castable materials, films and tapes, sprayable coatings, and two component, room temperature curing systems. In total, 74 material configurations were tested for rain erosion resistance at a whirling arm rain erosion test rig located at Wright Patterson Air Force Base, Ohio. The top candidate material proved to be a moldable aliphatic polyether TP urethane from 3M Corporation. It proved to last 36 times longer than an uncoated glass/epoxy reference sample and almost four times longer than the next best performing material.

In summary, there exists a substantial amount of experimental data on the performance of composite materials in a rain erosion environment. Given the similar damage mechanisms to that of cavitation erosion, perhaps some of the same materials and techniques that are effective in increasing a material system's rain erosion resistance will also be effective in increasing a material's cavitation erosion resistance. For uncoated composite material systems, the use of multidirectional reinforcements with fibers oriented through the thickness appears to be the best design alternative for the current application. This however may add significant material complexity and may not be feasible given a suitable alternative such as elastomeric materials.

2.5 Previous Composite Material Testing for Cavitation Erosion

As stated previously, most of the erosion studies done on GRP materials focus on the rain erosion resistance of these materials. The body of literature that specifically examines

the cavitation erosion resistance of GRP materials is considerably smaller. Two of the cavitation studies of interest will be reviewed in this section. The first is entitled "Cavitation Erosion Performance of Fiber Reinforced Composites" by Douglas Hammond from Pennsylvania State University [Hammond et al., 1993]. This work served as the basis for much of the research relating to composite materials that is contained herein. In this study, the authors investigated four different fiber/resin combinations utilizing carbon and glass fibers as well as both epoxy and thermoplastic resins. The test method was based on a modified ASTM G32 vibratory induced cavitation method. The results from this study show that all the different GRP materials perform similar to one another in their cavitation erosion resistance. By comparison, the GRP materials perform better than aluminum, but not as good as NiAl bronze. The authors discuss in detail the damage mechanisms of the composite substrate. Scanning electron microscope pictures of the cavitated surface show that the early damage mechanism is a general erosion of the outer matrix material that covers the fibers. Once the fiber reinforcement is exposed, the anisotropic nature of the composite begins to have an effect on the erosion patterns. The softer matrix material is eroded in between the fiber bundles and provides for what the authors describe as a tunneling or wave guide effect for the cavitation bubbles. This effect serves to undermine the stiffer fiber bundles and ultimately leads to fiber breakage and erosion. It is noted in this report that although composite materials are generally more compliant in their transverse material stiffness compared to metallics, traditional layup geometries only serve to reduce the cavitation forces by 15-20 percent. In general, this paper concludes that composite materials are not as good in cavitation erosion resistance as more traditional metallics. Noted as an

exception to this conclusion, however, was a study performed by Djordjevic and co-workers [Djordjevic et al., 1988]. They examined composite materials with a sandwich construction in order to more suitably tailor the transverse stiffness of the material. The tested materials contained either one or two layers of E-Glass/Epoxy over a PVC foam core. Results from the testing using a similar vibratory induced cavitation method showed that the single laminate construction over a foam core yielded less erosion than stainless steel. One interesting element from the testing was the reporting of combustion of the foam core due to excessive heat buildup from the energy absorption. The authors report that by inserting steel wires into the foam core, the thermal conductivity of the foam was increased sufficiently to stop the reported combustion during testing. Although the favorable results of this testing is unique in the literature, the ability to tailor the transverse material properties of composites using sandwich construction and energy absorbent core materials is an advantage when considering how to protect composite panels from the cavitation environment. For this reason, an effort was made during this testing to duplicate these results and explore the potential of this material system.

3. Erosion Resistant Material System Considerations

The cavitation erosion resistant material system used in the underwater lifting body is intended to be a nonstructural outer layer of the composite substrate. Figure 3.1 schematically shows a number of different potential material systems investigated. These include a durable composite outer skin with or without an energy absorbing core material (Figure 3.1a), a durable composite skin with a thin layer protective coating (Figure 3.1b), and a metal or elastomeric skin applied directly to the structural composite substrate (Figure 3.1c). These material systems are arranged in their relative order of risk versus reward based on potential nonstructural weight added to the system, compatibility and post lay-up manufacturing considerations. It is generally agreed that a durable composite material system will be the most difficult to realize when compared to more traditional metallic solutions yet it will offer the greatest potential rewards with respect to weight savings.

Based on a review of the cavitation erosion mechanisms and a review of the use of composites in the marine industry, a number of material systems were selected for design, construction and testing. When evaluating GRP composites, Figure 3.2 summarizes a qualitative ranking of various material constituent properties [Greene, 1999]. Given this summary of materials and the Navy's guidance with respect to applicable GRP material selections, specific combinations of fiber, matrix and core were manufactured and tested. As with any experimental effort, lessons and results learned in this first round of testing were incorporated into future testing and material system consideration.

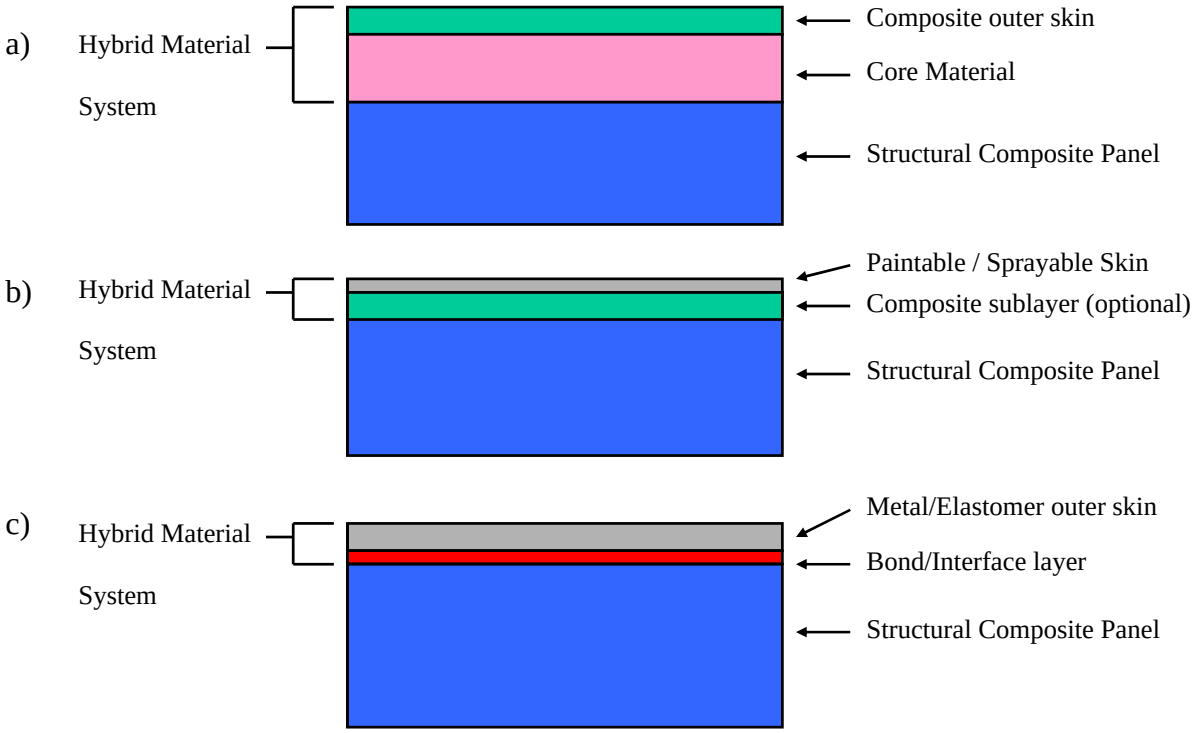

Figure 3.1 – Schematic representation of different types of material systems

	Fiber			Resin					Core					
	E-Glass	Kevlar	Carbon	Polyester	Vinyl Ester	Epoxy	Phenolic	Thermoplastic	Balsa	Cross Link PVC	Linear PVC	Nomex/Alum Honeycomb	Thermoplastic Honeycomb	Syntactic Foam
Static Tensile Strength	■	■	■	□	□	■	□	□	■	■	■	□	□	□
Static Tensile Stiffness	□	■	■	□	□	□	□	□	■	□	□	■	□	□
Static Compressive Strength	■	□	□	□	□	□	□	□	■	□	■	■	□	□
Static Compressive Stiffness	□	□	■	□	□	□	□	□	■	□	□	■	□	□
Fatigue Performance	□	■	■	□	■	■	□	■	■	□	■	□	■	□
Impact Performance	■	■	□	□	■	■	□	■	□	■	■	□	□	□
Water Resistance	■	□	□	□	■	■	□	■	□	■	■	□	□	□
Fire Resistance	■	□	□	□	□	□	■	□	■	□	□	■	□	□
Workability	■	□	□	■	□	□	□	□	■	□	□	□	□	■
Cost	■	□	□	■	□	□	□	■	■	□	□	□	■	■
	■ Good Performance □ Fair Performance													

Figure 3.2 – Qualitative assessment of marine composite construction materials [Greene, 1999]

3.1 Composite Erosion Protection System

Six different composite material systems were developed for study using carbon, E-glass and quartz fibers. In addition to testing the base E-glass structural material system, a pure carbon fiber/vinyl ester laminate was also tested. Building from the concept depicted in Figure 3.1a, three different combinations of materials and foam core were tested. These samples included single layers of carbon, quartz, and a unique carbon/quartz hybrid fabric all bonded to a linear PVC foam core. A number of sprayable/paintable elastomer coatings were also tested based on Figure 3.1b. In addition to the composite and elastomer material systems, a number of metallic solutions was also investigated as potential candidates for thin skin material as shown in Figure 3.1c. The specific properties of these composite material systems and the rationale for their selection are presented in this chapter. Material selection was based upon materials that are typically used for marine structural purposes. It is noted that good structural properties and cavitation erosion resistances are not necessarily correlated.

3.1.1 Fiber Properties

The selection of fiber types for testing was based on a review of recent marine industry practices of both recreational and commercial vessels as well as input from U.S. Navy composite designers. The fiber types investigated provide a broad range of physical properties in order to tailor the end structural properties and are all compatible for use in the marine environment. The mechanical properties of each fiber type are listed in Table 3.1. When applicable, a particular grade or subtype of fiber has been specified. From

this comparison, it was decided to investigate both glass type and carbon fibers. These two choices provided the full range of strength, stiffness and strain at failure properties. The actual laminate weave and ply schedule will be discussed in Section 3.2.3. The addition of High Purity Quartz Yarn (HPQY) was made at the manufacturers request because of availability. Its properties were considered to be very close to E-glass when tested. Although aramid fibers are widely known for their impact resistance, they were not included as part of this test sequence due to their hydrophilic nature.

Table 3.1 - Fiber property comparison

	E-Glass	**HPQY**	**Aramid Kevlar® 49**	**Carbon T300**
Density (lb/in^3)	0.094	0.079	0.052	0.064
Tensile Strength (ksi)	500	400	522	529
Tensile Modulus (Msi)	11	10	19	33.5

3.1.2 Resins

The resin selection was based on a review of the compatibility with the fiber and the marine environment. Table 3.2 presents properties of the resins evaluated under this effort and includes three versions from the DOW Derakane™ family. Derakane™ 8084 was selected for the testing both because of its interest to the Navy and its extensive use in the structural tests performed under the MACH program. It is a rubber-modified version of the base Derakane™ family with greater elongation and impact resistance. All of these resins are reported as having good properties with respect to strength, fatigue and energy absorption.

Table 3.2 - Resin property comparison

	Derakane™ 411-350	**Derakane™ 8084**	**Derakane™ 510A**
Viscosity	350 cps	350 cps	350 cps
Specific Gravity	1.13	1.13	1.23
Tensile Strength	11,500 psi	10,500 psi	10,500 psi
Tensile Modulus	490 ksi	460 ksi	500 ksi
Tensile Elongation	6.5 %	11 %	5 %
Flexural Strength	17,000 psi	17,000 psi	18,000 psi
Flexural Modulus	450 ksi	440 ksi	530 ksi
Reverse Impact	57 in-lb	207 in-lb	

3.1.3 Sandwich Core Materials

The sandwich core selected for investigation has a good mix of strength and energy absorption properties along with good fatigue performance. The core material selected was the Airex R63.80 linear PVC foam from Baltek Corporation. Its properties are compared to a common end grain balsa in Table 3.3. Polyvinyl foam cores are manufactured by combining a polyvinyl copolymer with stabilizers, plasticizers, crosslinking compounds and blowing agents. The mixture is heated under pressure and then submerged in hot water tanks in order to expand to the desired density. The material is generally available in either a cross-linked or linear form. Linear PVC foam has a non-connected molecular structure that allows significant internal displacement of the material before failure which results in the high energy absorption characteristics of the material [Greene, 1999]. This is illustrated in the higher impact strength rating and the greater shearing at break percentage listed in Table 3.3. Although a common core material for hull structures, balsa was not considered for this study due to the Navy's hesitation about its use below the waterline.

Table 3.3 - Core material property comparison (properties courtesy of Baltek Corporation)

		Linear PVC	**Cross-linked PVC**	**End Grain Balsa**
Product Designation		**Airex® R63.80**	**Airlite™ C70B-5.0**	**Superlite™ S56**
Nominal density	kg/m3	90	86.5	97
	lb/ft3	5.6	5.4	6.07
Compressive strength Perpendicular to plate	psi	130	169	961
Compressive modulus Perpendicular to plate	psi	8120	9238	302664
Tensile strength In plane	psi	200	334	1114
Tensile modulus In plane	psi	7250	18625	
Shear strength	psi	145	181	271
Shear modulus	psi	3050	3580.5	15696
Shearing at break	%	75	25	
Impact strength	lb-ft/in^2	2.4	0.53	

3.1.4 Laminate Geometry

The laminate geometry implies a mixture of ply thicknesses (thick or thin), ply orientations and weave geometry. Figure 3.3 depicts typical weave patterns for composite fabrics. The custom weaves used in the carbon fiber, HPQY, and combination carbon/HPQY were all harness weaves as depicted in (d). Specifics of the various laminate geometries are listed in Table 3.4. As cited by Hammond, the common failure mechanism for composites is the erosion of the matrix around the fiber bundles which eventually leads to subversion and fiber breakage. It is possible that different weave densities and/or geometries could influence this behavior by more closely packing the fiber reinforcement. Although this methodology was not specifically tested during this study, inherent size differences of the different fiber bundles does provide some empirical

evidence based on weave density alone. A full discussion of the material systems and their results is given in Chapter 5.

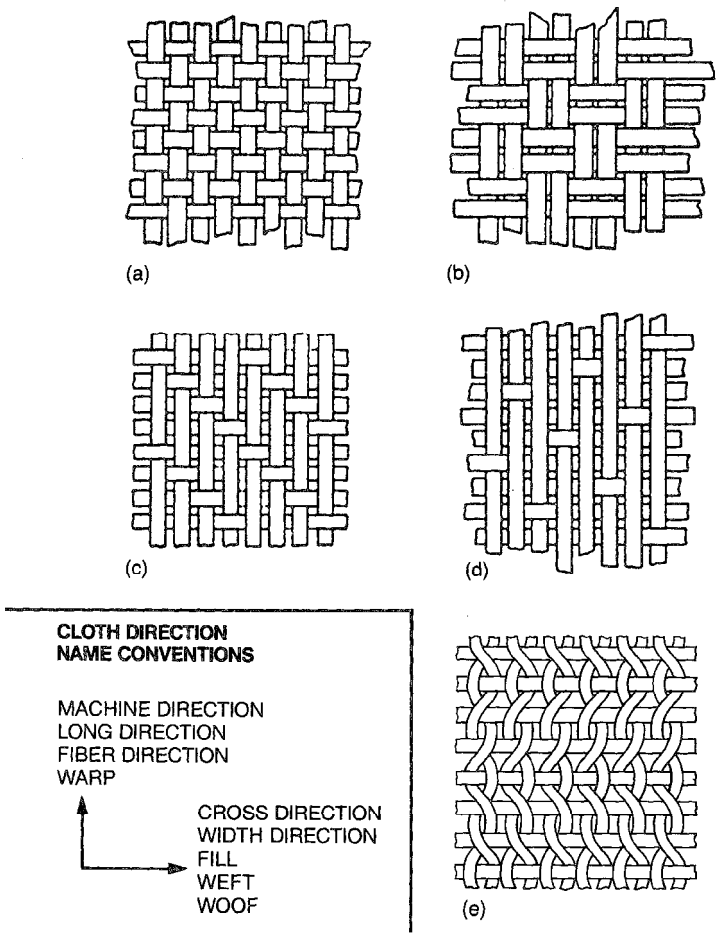

Figure 3.3 - Laminate weave geometries [Strong, 1989]

Table 3.4 - Manufactured laminate geometries

	Fiber (warp/fill)	**Weave density (picks/inch) (warp/fill)**	**Fabric weight (oz/yd)**	**Ply thickness (mils)**
Fabric A	T300-3k/T300-3k	24/23	10.7	11
Fabric B	HPQY/HPQY	54/55	9.5	9
Fabric C	T300-3k/Quartz 300 2/2	24/60	10-13	12-14
Fabric D	E-glass	NA	24	31

3.2 Surface Protection Layers

In addition to the foam core composite material system, a number of different surface coatings were also investigated. The two classes of coatings investigated were hard ceramic coatings and energy absorbing polymers/elastomers. Hard ceramic coatings are often used in the protection of metallic components in cavitating environments such as the turbine blades in a hydroelectric turbine. The Army Corp of Engineers in conjunction with the Tennessee Valley Authority conducted a fairly thorough review of these coating options [Boy et al., 1997]. One drawback of many of these materials is the application method. A majority of these coatings are applied with either plasma spraying or HVOF (high velocity oxy fuel) techniques. Both of these techniques impart a good deal of thermal loading onto the substrate surface during application. Given the low temperature limitations of a composite substrate, these techniques were avoided. There are however, a few ceramic coatings that are applied with a brush or other similar methods. One such coating is CeRam-Kote manufactured by Freecom, Inc. This coating was included in the testing on the recommendation of Navatek. They have used this coating on previous vessels with good results. The bulk of the testing involved various polymer/elastomer formulations. Many of these coatings are applied either by brush or low pressure spraying and are thus suitable to large scale composite structures. These materials included silicone rubbers, urethanes, fluoroelastomers and polyurea compounds. There were also some materials included that are applied in a sheet form. These included EPDM rubber and SCAPA® tape which is most commonly used as an erosion shield on the leading edges of propellers and helicopter blades. A full list of the elastomer materials tested is given and discussed in Chapter 5.

3.3 Metal Skins

The third material system concept depicted in Figure 3.1c consists of a thin metal skin applied over the base structural composite. Materials considered for this protection system included NiAl bronze (propeller bronze), 316L stainless steel and two highly corrosion resistant duplex stainless steels, ferralium (alloy 255) and Zeron® 100. Ferralium is a high strength, corrosion resistant stainless steel produced by Langley Alloys of Staffordshire England. Zeron® 100 is a similar grade of material produced by Weir Materials and Foundries in Manchester England. Drawbacks to the implementation of this system include the added weight, formability concerns with complex curves and the difficulty of adequately bonding the metal to the composite substrate. No specific testing or evaluation was undertaken to evaluate these factors. If this type of system were implemented, it is most likely that these metallic protection panels would only be applied to the areas most prone to severe cavitation attack. The results for these materials are given in Chapter 5.

4. Cavitation Testing

The cavitation erosion testing of material system specimens is performed in accordance with a modified ASTM G32-98 standard. ASTM G32-98 is the "Standard Test Method for Cavitation Erosion Using Vibratory Apparatus". The ASTM G32-98 test procedure uses an ultrasonic horn to vibrate a test material placed in a liquid. It was necessary to modify the standard procedures during this research effort to allow for proper support of the material being tested. In the G32 standard, the material to be tested is fabricated to specific dimensions and threaded into the end of the ultrasonic horn. The test sample is then vibrated and the cavitation damage occurs on the under side of the sample. This mounting method presents a significant challenge when testing composite or elastomeric materials. A common modification to the standard test method used in previous studies such as those conducted by Hammond [Hammond et al., 1993] and Djordjevic [Djordjevic et al., 1988] is to mount the test sample stationary below the vibrating horn tip. The amplitude of the horn tip oscillation as well as the horn tip to sample distance is carefully controlled in order to assure a repeatable test environment. Although the cavitation erosion mechanism present in this method is not the same as that on an immersed moving body, this method has been shown to be useful in ranking various materials with respect to their erosion resistance. Given the minimal equipment required and the simplicity of the test method, it is an attractive method for providing valuable data for a proof-of-concept study where the erosion resistances of new material systems are compared to traditional materials on a relative basis.

4.1 Test Apparatus

The ASTM G32-98 test method utilizes a commercially available ultrasonic transducer, which is attached to a tuned "horn" oscillating at 20 kHz. The particular ultrasonic equipment used is a Branson Ultrasonic Digital Sonifier model S450D as shown in Figures 4.1 and 4.2. The replaceable horn tip is constructed of Ti-6Al-4V. The tip of the

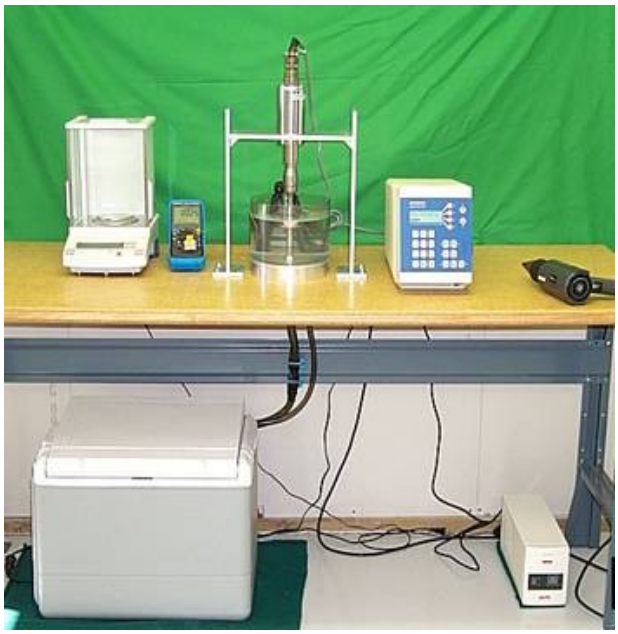

Figure 4.1 – Photograph of the experimental test apparatus

Figure 4.2 – Close-up photograph of the specimen holder

horn oscillates above the test sample at a precisely controlled distance and produces cavitation bubbles that impinge on the surface. The peak-to-peak tip displacement is OEM calibrated and adjustable on the amplifier. It is set to 0.050 mm for these tests. The test sample is mounted 0.50 mm away from the oscillating tip. Bulk fluid temperature in the container is maintained at 23-27º C by the use of a cooled water recirculation system. The temperature is monitored by a thermocouple in the tank. The erosion rate of the material is determined by periodically stopping the test and drying and weighing the sample. Weight was taken using an Ohaus Adventurer scale that has a 65g capacity and a precision of 0.0001g. The testing method is calibrated periodically using standard 6061-T6 Aluminum or Ni 200 as a reference material.

4.2 Test Method

The following procedure has been adapted from ASTM standard G32-98. This represents the current test procedure used for each specimen:

1. Clean test vessel, specimen stand, and cooling pump.
2. Clean, dry, and weigh the horn tip.
3. Attach horn tip as specified by the product manual.
4. Fill test vessel and cooling pump with fresh liquid.
5. Obtain a 1”x1”x1\4” thick (approximate) specimen. Machine and polish a 1”x1” surface so that neither pitting nor scratches are visible (metal samples).
6. Weigh the specimen before cleaning.
7. Record pre-clean mass.

8. Clean, dry, and weigh the specimen.
9. Record post-clean mass.
10. Determine if more drying time is necessary. If mass has increased since pre-clean mass then sample is absorbing water from the cleaning process. Porous materials like composites are notorious for this.
11. If more drying time is necessary chose a drying technique based on material and time requirements. Common drying techniques include room-temperature drying/stabilizing and drying with heat lamp. Heated drying accelerates the stabilization time, but may not be suitable for all materials. Heated drying was used for this study due to time requirements.
12. Weigh specimen at 1 hr intervals. If the specimen mass is consistent for 2 consecutive readings then the mass has stabilized.
13. Record the mass, test material (first time), and elapsed time.
14. Secure the specimen to the test stand.
15. Locate the horn tip 0.5mm above the specimen and secure in place.
16. Measure the liquid height in the vessel. The liquid height should be at least 100mm and the immersion depth of the specimen should be 12mm ± 4mm. Adjust the liquid level as needed.
17. Power up the Digital Sonifier. Set the interval time and horn amplitude. Refer to the ASTM standard for approximate interval times. Refer to the product manual for amplitude settings. For this test the tip-to-tip displacement is 50 microns.
18. Start the test.
19. Monitor the liquid temperature and use cooling as needed.

20. At the end of the interval, clean, dry, and weigh the specimen.
21. Repeat step 11 and 12 until mass stabilizes.
22. Record mass and elapsed cavitation time. Repeat steps 11 through 19, omitting 12, 13, and 14, until two successive weighings yield identical (or acceptably similar) readings.

4.3 Reduction of Test Results

Interpretation and reporting of cavitation erosion test data is made difficult by two factors. The first is that the rate of erosion (material loss) is not constant with time, but goes through several stages. This makes it impossible to fully represent the test result by a single number, or to predict long-term behavior from a short-term test. The second is that there is no independent or absolute definition of "erosion resistance", nor can units of measurement be ascribed to it. The following paragraphs describe the suggested data interpretation steps. A complete discussion of these issues can be found in the ASTM G32 standard.

The primary result of an erosion test is the cumulative erosion-time curve. Although the raw data will be in terms of the mass loss versus time, for analysis and reporting purposes this should be converted to a "mean depth of erosion" (MDE) versus time curve, since a volumetric loss is more significant than a mass loss when materials of different densities are compared. The MDE is calculated by dividing the mass loss measured by the density of the material and the affected cavitation area. For comparisons, the cavitated area is

considered to be the horn tip area and for this setup is 0.866cm^2 (0.1342in^2). Thus MDE is given by Equation 4.1.

$$MDE = \frac{\Delta mass}{\rho * Area} \tag{4.1}$$

A typical MDE curve from a metallic sample is shown in Figure 4.3. Given the shape of the cumulative erosion-time curve, it is not meaningful to compare the absolute MDE for different materials after the same exposure time. The reason is that a selected time may still be within the incubation or acceleration stage for a very resistant material, whereas for a weak material the same time may be within the maximum rate or deceleration stage. The most common single-number for comparison of different materials is the maximum rate of erosion. This can be defined as the slope of the straight line that best approximates the linear, (or nearly linear) steepest portion of the MDE curve and is expressed in micrometers per hour.

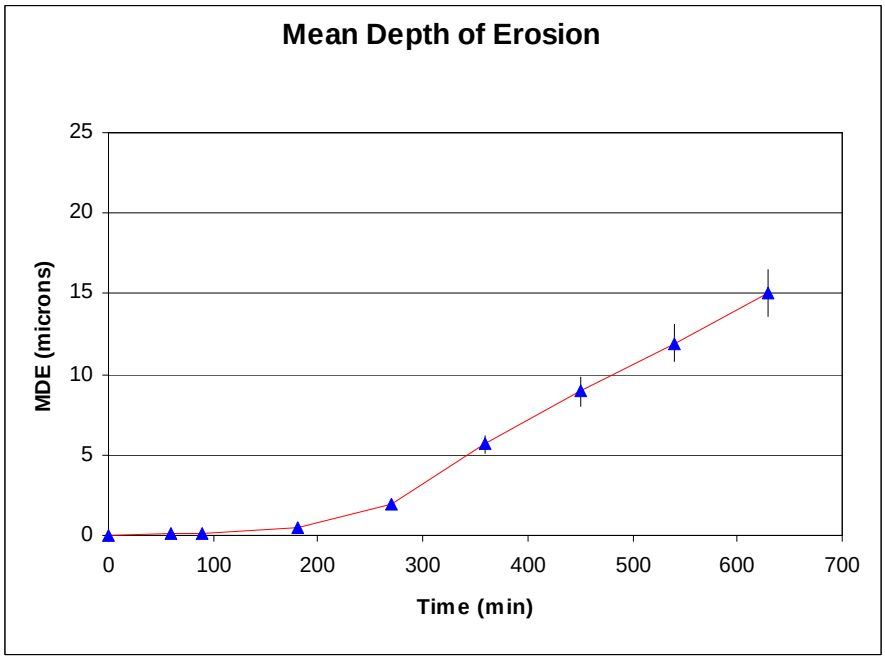

Figure 4.3 - Example Cumulative Erosion-Time Curve

Care should be taken not to extrapolate a material's cavitation resistance in the G32 tests to some in-service condition. The nature of cavitation and its effects on structures depend on a number of factors some of which are not fully understood. Thus any G32 testing merely represents a relative ranking of a material's cavitation erosion resistance when compared to a reference material of interest.

4.4 Calibration of Test Setup and Procedures

The ASTM G32 standard recommends calibrating the test apparatus and procedures using a Nickel 200 material and comparing the results with those provided in the standard. The standard lists results from five independent labs and these are shown in Figure 4.4. The error bars on the curves represent a single standard deviation.

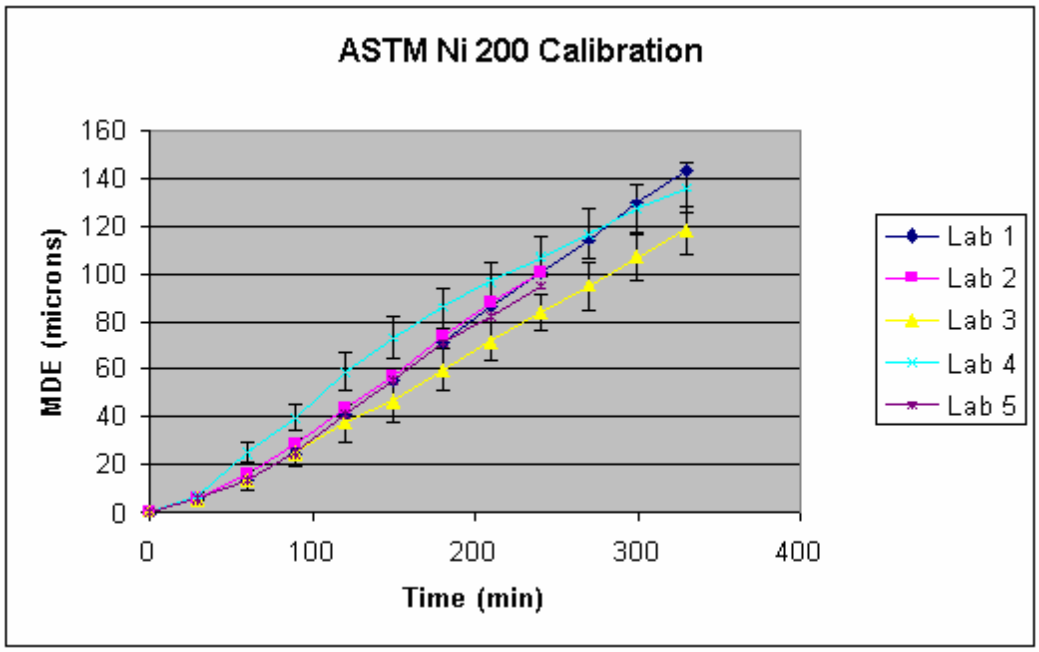

Figure 4.4 - MDE for Ni 200 from independent lab tests using ASTM procedures

The results of testing Nickel 200 with the modified procedures are presented in Figure 4.5. Also plotted are the erosion rate results from the calibration lab data. This plot highlights a discrepancy in the data between the two methods. Although the data from the modified test method appears to be repeatable between tests, the erosion rates calculated are much lower than those provided by the ASTM standard data. Several reasons for these discrepancies have been identified. The area of the cavitating horn tip in the standard is larger by a factor of 2.3 than that used in the modified test. The tip area will affect the overall mass loss area and thus the reported quantity of MDE. In an effort to account for this difference, the results for the calibration tests have been normalized with respect to tip area and are compared in Table 4.1. The results show that the

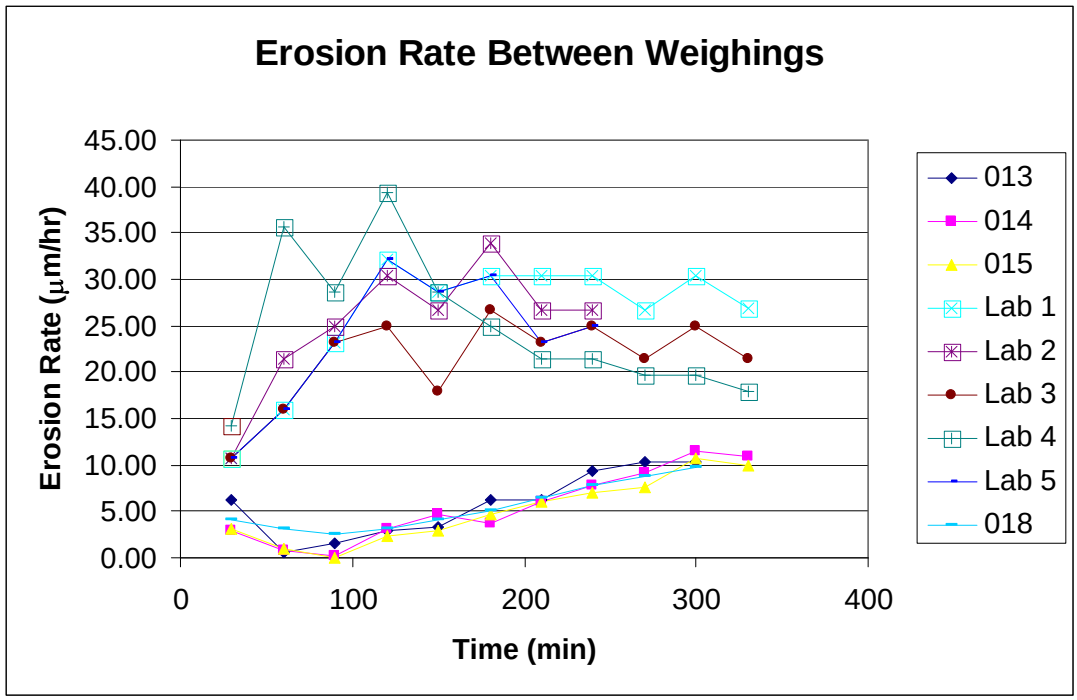

Figure 4.5 – Erosion rate of Ni 200 samples Using Modified Procedures

normalization process provided starting values of MDE that are comparable; however, the results from intermediate times vary significantly. Part of this trend can be attributed to the drop in erosion rate of our test samples shown in Figure 4.5. The difference in horn tip area could also cause a difference in cavitation intensity under the horn. As outlined in the theory section, the force imparted on a substrate by a cloud of bubbles is much greater than the force from a single bubble. Given this behavior, it does not seem unreasonable that the cavitation cloud under a larger horn tip may be more intense and result in more damage to the material. It is also possible that an unidentified material discrepancy exists in the tested nickel samples. In any case, further efforts to correlate data between the modified testing method and that of the standard method were not pursued. The following section will discuss the repeatability testing that was done on the modified testing method. Given the fact that this effort seeks to rank each material's relative erosion rate, it was determined that repeatability of the method was the most important aspect of the test method.

Table 4.1 – Comparison of normalized MDE for Ni 200 Standard versus Modified Procedure

	ASTM Independent Test Labs					
Time	Lab 1	Lab 2	Lab 3	Lab 4	Lab 5	Calibration Test
(min)	MDE / inch^2					
0	0	0	0	0	0	0
30	17.52692503	17.52693	17.52693	23.34743	17.52693	15.51805
60	43.78461308	52.54808	43.78461	81.74872	43.78461	23.27707
90	81.74871748	93.42243	81.74872	128.4763	81.74872	29.09633
120	134.2967931	143.0603	122.6231	192.6654	134.2968	46.55414
150	181.02436	186.8449	151.8237	239.3929	181.0244	76.62035
180	230.6621812	242.3359	195.6083	280.2673	230.6622	111.536
210	280.267303	286.1205	233.5724	315.3212	268.5936	167.7889
240	329.9051243	329.9051	274.4468	350.3423	309.4679	229.861
270	373.6897374	NA	309.4679	382.4532	NA	294.8429
300	423.3275586	NA	350.3423	414.5641	NA	360.7946

4.5 Repeatability of Modified Test Using Aluminum Samples

Since current testing focuses on obtaining relative rankings of cavitation resistance, repeatability was determined to be more critical than the ability to correlate test data with data found in published sources. 6061-T6 aluminum was chosen as the standard for checking the consistency and repeatability of the test method because of its higher availability and shorter test times than Nickel 200. Figure 4.6 shows the cumulative mean depth of erosion (MDE) curves for multiple aluminum samples. As can be seen from the plot, all test data points are within one standard deviation of each other as shown by the error bars. By periodically running one of these samples throughout the testing, it is ensured that the test apparatus and test method remain reliable and provide consistent relative data for the erosion rate of different materials systems.

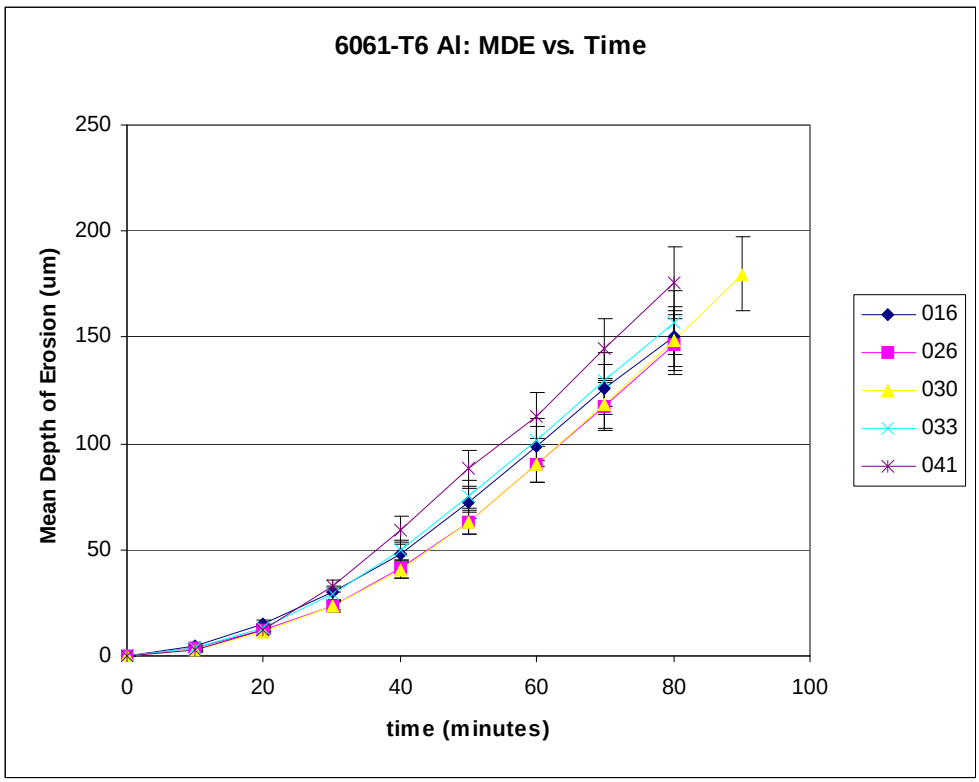

Figure 4.6 – Repeatability of 6061-T6 Aluminum Samples

4.6 Addition of Data Acquisition System for Overnight Testing

The long test times of EPDM rubber and other durable elastomer samples created a need for overnight testing capability. In the original test setup, overnight testing was not possible because tank temperature monitoring was done by hand periodically and the cooling pump was turned on manually when needed (often several times on warm days). In order to keep the tank temperature between 23-27ºC as recommended by the ASTM G32-98 standard, the thermocouple was attached to an IOTech™ data acquisition system, allowing the temperature to be monitored using a custom written LabView™ program. The cooling pump was attached to a solid-state relay that was switched on when the temperature exceeds the threshold and switched off when the tank has cooled. This system has provided repeatable results for long test intervals.

5. Discussion of Test Results

This chapter highlights the results of the cavitation testing for each of the material classes. Following ASTM guidelines, the maximum erosion rate was used as the parameter to relatively rank each material. As discussed in Section 4.1.3, the maximum erosion rate represents the maximum slope in the mass loss versus time curve and is calculated using Equation 4.1. The maximum erosion rate values presented represent the average erosion rate of at least two independent tests whenever possible. A summary of the results from the testing can be found in the Appendix. A complete data set is available upon request. Non-metallic samples often presented challenges in obtaining repeatable data. The hygroscopic nature of composites and some elastomers made the drying process difficult and often required excessively long drying times during the weighing process. These challenges will be discussed further during the following sections.

5.1 Metals

There exists a vast amount of data on the erosion resistance of various metals. Although the use of a metallic skin was presented as a potential material system, an exhaustive search of all applicable materials was not considered within the scope of this study. Instead, the materials chosen for testing serve to baseline the testing method and apparatus when compared to the composite and elastomer material systems of interest. It is anticipated that if a metallic material system were chosen for implementation, a thorough investigation into the various alloys would be conducted before a material selection was made. In this report, results will be presented for Aluminum 6061-T6

which was used primarily to periodically calibrate the test setup. The reference material for comparison of erosion resistance was chosen to be 316L stainless steel. This steel is often used in cavitating environments including turbine blades, valve and piping components. It is generally considered to have a high resistance to cavitation erosion, thus any new material system should show results close to or better than this material. NiAl bronze was also tested as a reference material given its history of application in cavitating environments. Three new metallic samples, ferralium, Zeron 100 and AL6XN, were also tested because of a lack of specific information on their cavitation erosion resistance in the literature. These materials were added to this study by specific request of Navatek and ONR. The erosion rate presented for titanium was calculated from data taken from the horn tip erosion and is reported for reference only. If considered, this material would need to be tested explicitly.

Figure 5.1 shows a plot of all the aluminum samples tested. Eliminating the highest and lowest values from tests #109 and #147 respectively, the average erosion rate is 152 μm/hr. It should be noted that test #041 and test #151 used opposing sides of the same sample. Very good agreement is shown in the erosion results between these tests. Figure 5.2 is a typical example of the excessive damage of aluminum samples. Given its low damage tolerance, this material would not be a good choice in a cavitating environment.

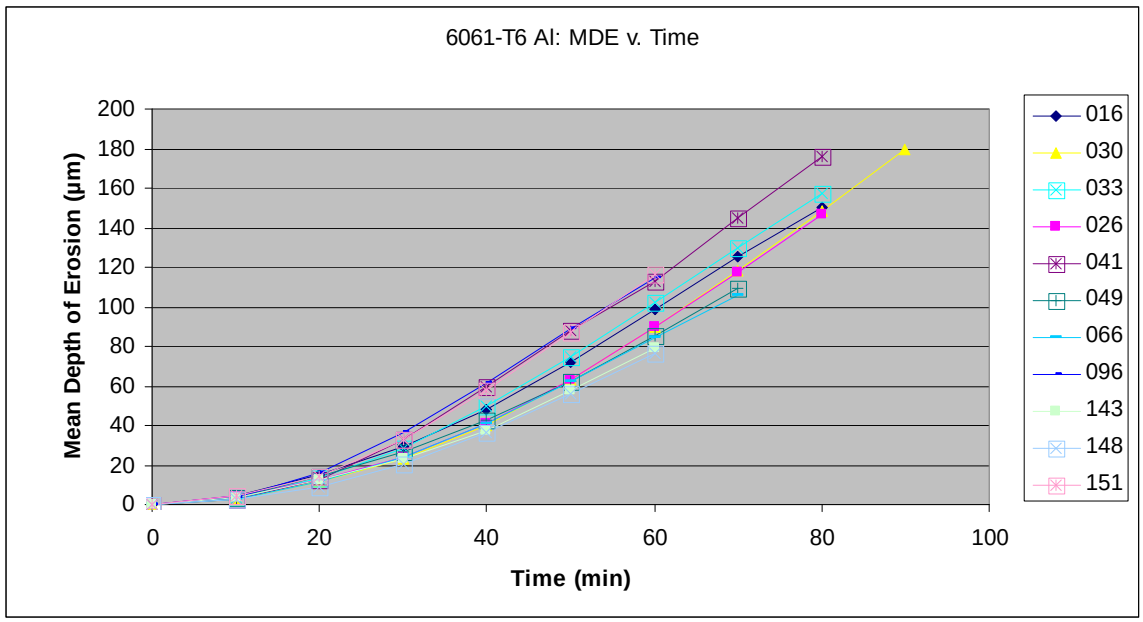

Figure 5.1 – Plot of MDE versus time for all Aluminum 6061-T6 samples

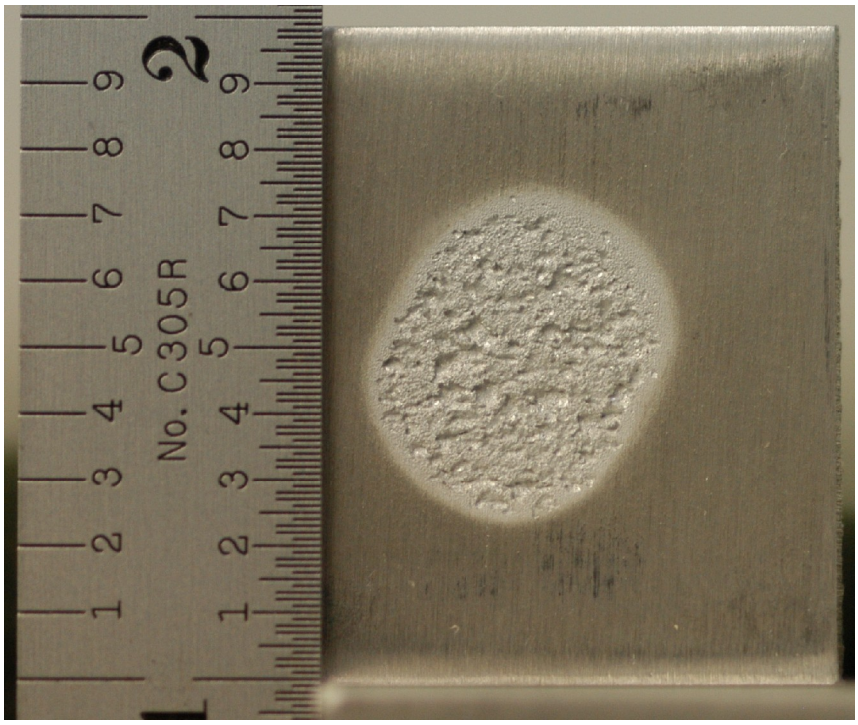

Figure 5.2 – Photograph of aluminum 6061-T6 sample #096 after testing

Figure 5.3 shows a plot of the three 316L stainless steel samples tested. Figure 5.4 shows the damage to sample #040 which is typical for these materials. When compared with the aluminum, the stainless samples exhibit much less pitting and less overall mass loss. The remaining structural materials, NiAl bronze, ferralium, Zeron 100, AL6XN and titanium all fall within 0.65 μm/hr of each other as depicted in Figure 5.5. Each of these materials shows similar damage patterns to that of 316L stainless steel. Based on this data, it appears that any of the stainless steels tested would provide a good cavitation erosion resistant material. If weight is a primary concern, then titanium may be a good choice.

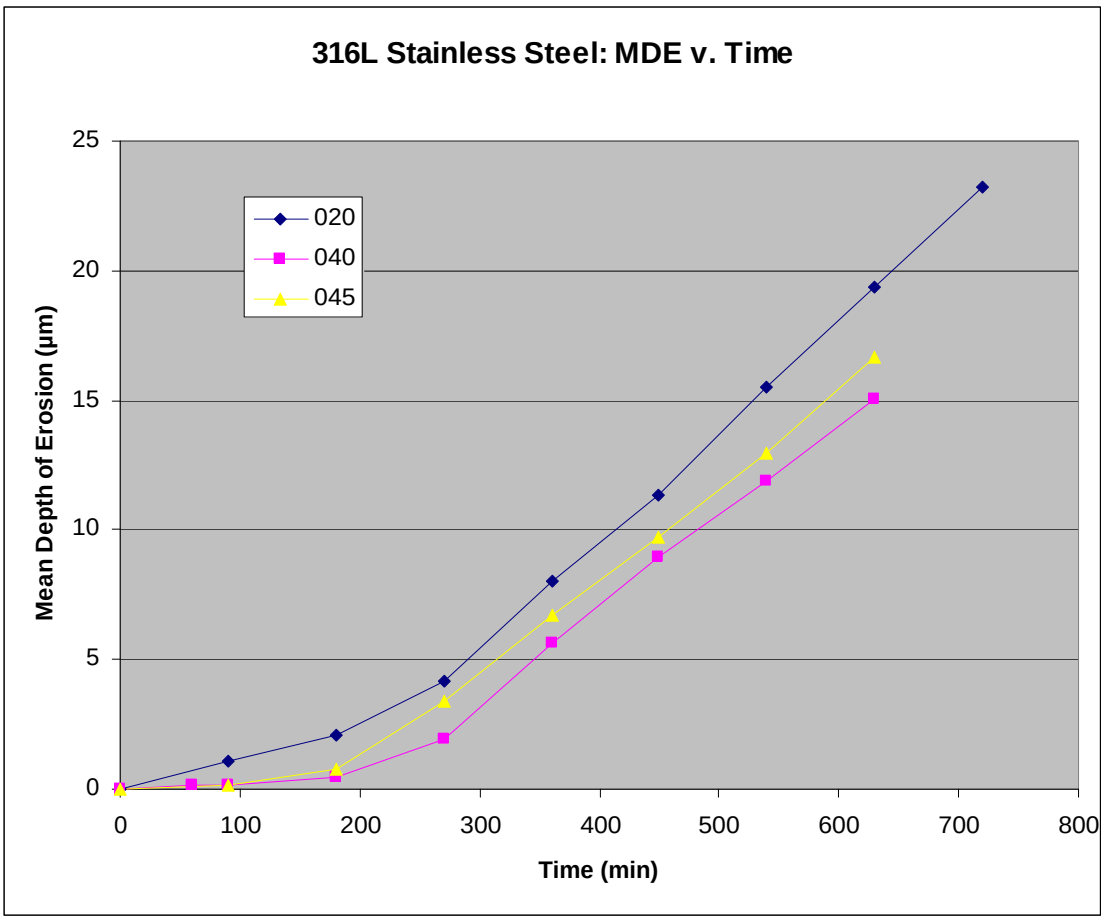

Figure 5.3 – Plot of MDE versus time for 316L stainless steel samples

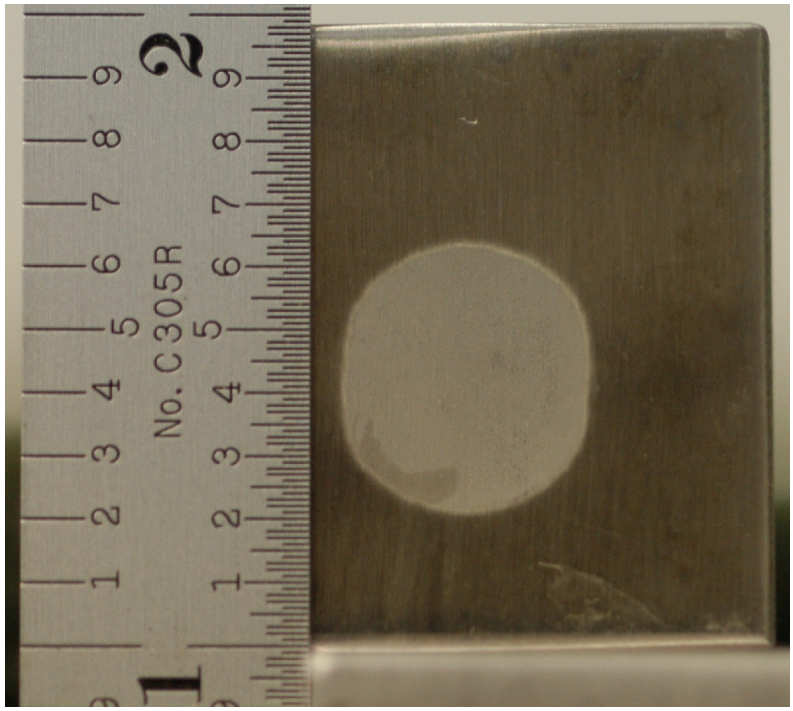

Figure 5.4 – Cavitation damage of a 316L stainless steel sample #040

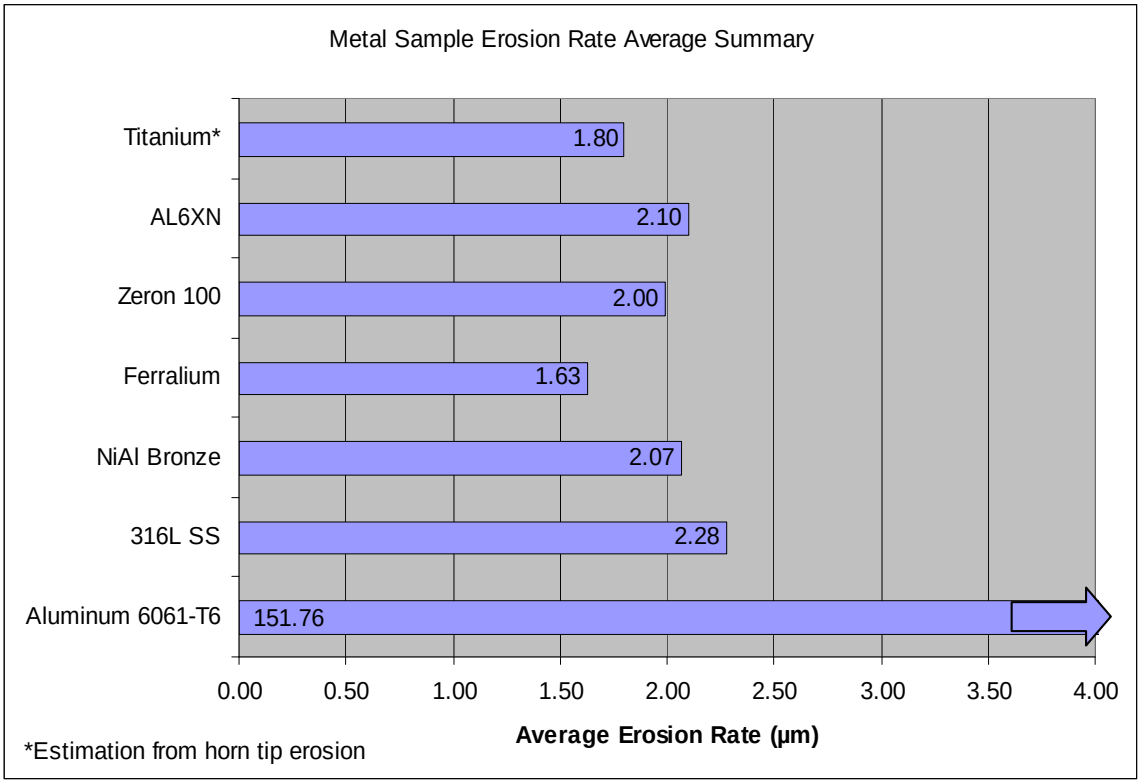

Figure 5.5 – Summary results of cavitation resistance of candidate metal samples

5.2 Composites

Composite material samples tested were a combination of composite laminates and sandwich construction. The first laminate was a T300-3K 8HS carbon fiber weave from Fiber Materials, Inc. The lay-up used for all test specimens is quasi-isotropic, $([(\pm 45)_f,(0/90)_f]_n)_S$, where n varies according to the panel thickness. The carbon fiber cloth was 10.7 oz/yd and was impregnated with Dow Derakane™ 8084, which is an epoxy vinyl ester resin. It was fabricated using a wet lay-up process with a vacuum assisted cure. The next two laminates used an E-glass fabric and Dow Derakane™ 411 and Derakane™ 8048 resins. They were fabricated at the Crosby Laboratory, University of Maine, using a VARTM process. The composite is reinforced with an E-glass knit cloth procured from Brunswick Technology, Inc. The cloth is either a 24 oz. 0/90 cross-ply, or a 24 oz. ±45 bi-axial. Sandwich core samples were fabricated with either a single layer of the aforementioned carbon fiber fabric or a high purity quartz yarn fabric, style 581, also from Fiber Materials, Inc. Each of these samples was laid over a Baltek Airex R63.80 linear PVC core and impregnated with Derakane™ 8048 resin using a VARTM process.

The search for a durable composite outer skin proved to be difficult. The primary mechanism of failure as discussed in Section 2.5 is matrix erosion followed by fiber damage. This damage mechanism is evident in Figure 5.6 regardless of fiber type. A summary of the erosion rate results for the composite samples is presented in Figure 5.7 and shows a wide range of values. The combination of carbon fiber and Derakane™ 8084 resin showed the worst results at 684 μm/hr. The choice of resin does have an

effect on the overall performance of the material as demonstrated by comparing an E-glass/Derakane™ 411-350 resin sample (445 μm/hr) with the same E-glass fiber impregnated with Derakane™ 8084 resin (252 μm/hr). Both the 411-350 and 8084 are vinyl ester resins; however, the 8084 is a rubber modified resin formulation with increased strain to failure capacity. As shown by Djordjevic [Djordjevic et al., 1988], the use of an energy absorbing core material greatly improved the erosion resistance of the samples; however, core damage was evident in these samples. Figure 5.8 shows the carbon fiber over core samples and Figure 5.9 shows the quartz over core. The discolored area is the core damage. Djordjevic reported the core damage as combustion due to the high energy absorption. To briefly test this theory, a piece of PVC core was heated with a propane torch. The resulting color of the melted core was different than that depicted in the figures. By heating the core material, it discolored into a dark brown area. This is markedly different than the purple discoloration in the cavitation samples. No chemical analysis was conducted on the core material to determine definitively if this discoloration was due to combustion or some other chemical reaction. Given that even the best of these materials is not as erosion resistant as 316L stainless steel and the difficulty in their implementation in the MACH panel joint areas, it was decided to not pursue any further development of composite materials systems.

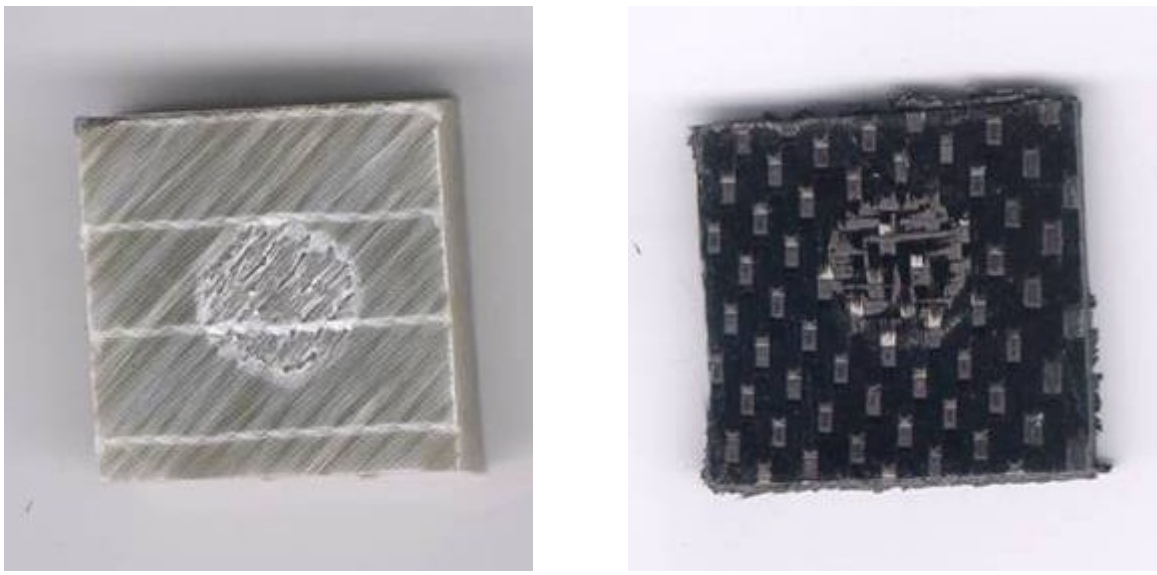

Figure 5.6 – Test sample of E-glass/8084 (left) and Carbon/8084 (right) showing matrix and fiber erosion

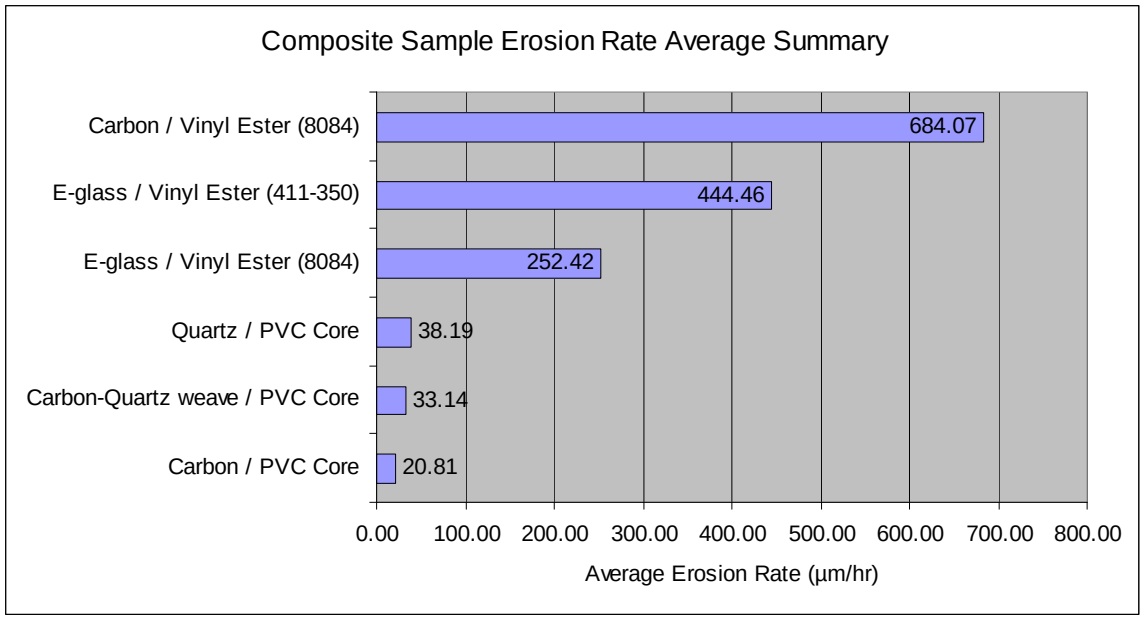

Figure 5.7 – Summary results of cavitation resistance of composite samples

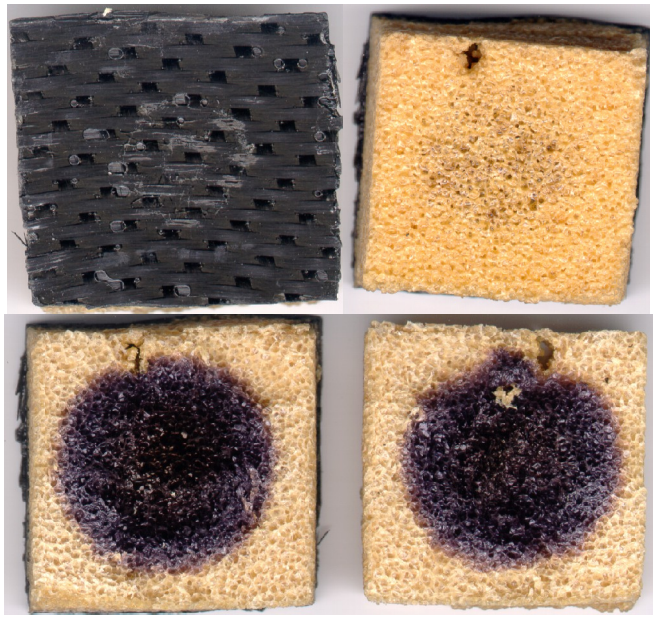

Figure 5.8 – Carbon fiber over PVC core samples showing core damage

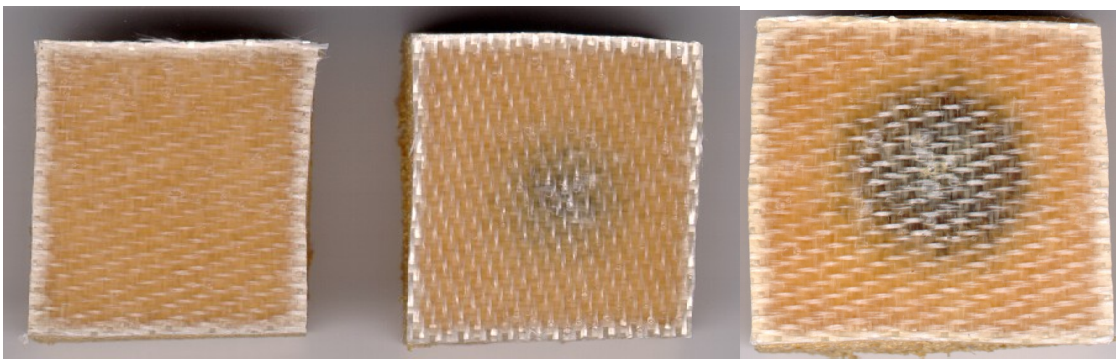

Figure 5.9 – Quartz fiber over PVC core sample showing core damage.

5.3 Elastomers

Elastomers are loosely defined as a group of materials characterized by the ability to resume their shape after being greatly deformed. They are natural or synthetic polymers and find primary uses in seals, adhesives and molded flexible parts. Common examples of elastomers include natural and synthetic rubber, silicone, neoprene, EPDM, polyurethane and many others. Because of their ability to absorb energy by elastic

deformation without failure, they were a natural class of material for investigation for cavitation erosion resistance. From the testing conducted during this effort, elastomer materials performed the best as a cavitation material solution that is equivalent or superior to stainless steel. As mentioned previously, there are thousands of elastomer formulations, each with unique properties. It was not within the scope of this study to investigate all elastomer based solutions. Often times, samples were merely screened for their total time to failure and failure mode in order to reduce the testing time due to the long drying cycles with these materials. Effort was made, however, to test different classes of elastomer materials. These results were then used to refine or expand the search within each class. The substrate for testing the elastomer samples was chosen to be aluminum instead of the E-glass composite. This was done because of the excessive drying times that were typical of the E-glass samples. Sheet elastomers were applied with a general-purpose two-part epoxy adhesive. Liquid formulations were applied to the manufacturer's specifications. Unless specifically noted, no accelerated cure heating was done to the liquid applications. Both commercially available products as well as specialty formulations were investigated. Each family of elastomers was evaluated based on its cavitation erosion resistance, failure mechanism, manufacturability, and pratical in-service applicability.

5.3.1 Ethylene Propylene Diene Monomer (EPDM) based Elastomers

The results from standard sheet EPDM rubber (0.72 μm/hr) show that the high elongation rates and high toughness of this material result in cavitation erosion rates that are about 3 times better than that of the 316L stainless steel reference material. The erosion curves

for samples #047 and #050 are shown in Figure 5.10. The peak erosion rate for these samples did not occur until more than 1500 minutes (25+ hrs) of testing had occurred. Even though the results from the sheet EPDM rubber appear to be good, the manufacturing concerns of bonding a complex geometry with a continuous sheet material prompted an investigation into a paintable or spray on formulation. There exist a number of liquid EPDM rubber variants that are applied with brushes or rollers and only require a room temperature cure. The sample chosen for testing was Liquid Rubber™ from Pro Guard Coatings. Pro Guard Coatings supplies the roofing and other industries with easy to apply rubber formulations. The test samples from both sheet and liquid EPDM rubber are pictured in Figure 5.11. It should be noted that the pictures show damage after only 122 minutes for the liquid EPDM. A total of 5 liquid EPDM samples were tested and only sample #080 provided a reliable erosion rate of (80 μm/hr). The other four samples experienced premature delamination or severe pitting damage and loss of material. Discussions with Hal Gouldner [Gouldner, 2002] of Pro Guard Coatings indicated that previous in-house testing of their liquid EPDM formulations also produced poor results. The reason that he gave related to the molecular and surface bond strengths being inadequate. The difference between their product and sheet EPDM is the amount of cross-linking present due to the curing process. The Liquid Rubber™ EPDM is a non vulcanized cure at room temperature. Vulcanization is a chemical process by which the monomer base chains of the material are cross-linked. It is often done at elevated temperatures and in the presence of other chemicals that provide the chemical cross-link between monomer chains [Bhowmick et al., 2001]. Sulfur is the most common cross-link

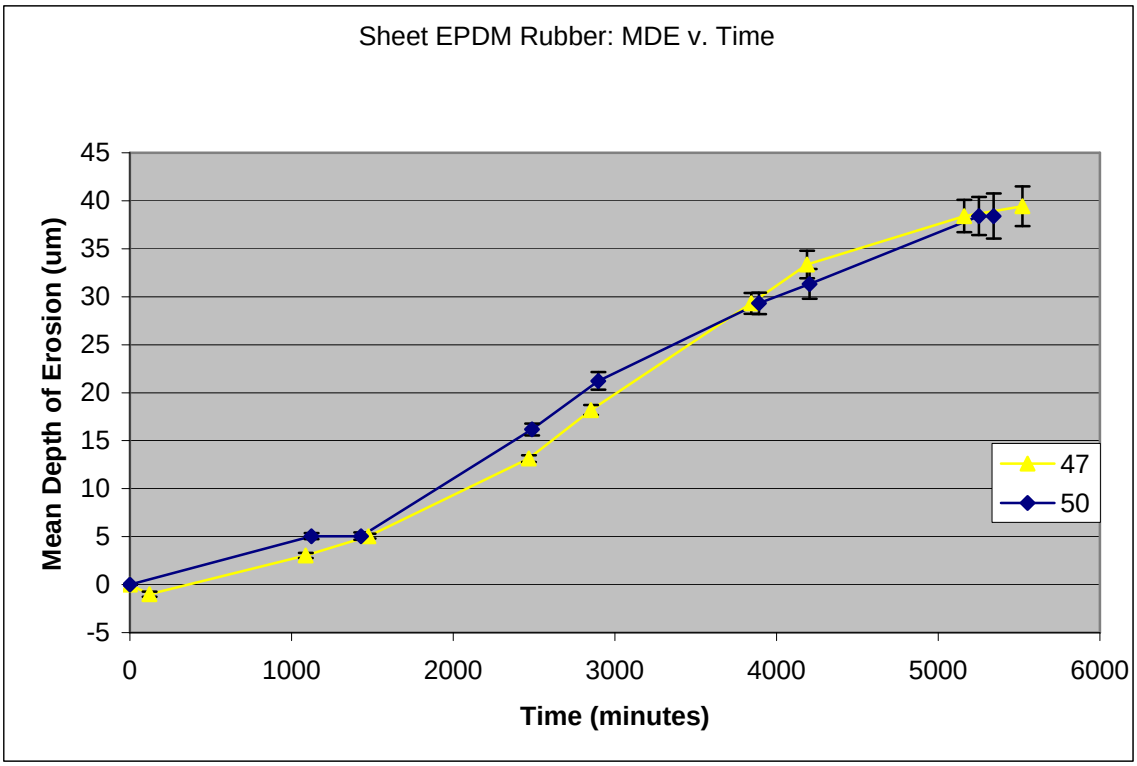

Figure 5.10 – Sheet EPDM results

material for EPDM rubbers. Most liquid EPDM formulations do not use a vulcanization process during the cure phase and thus end up with a lower cross-link density and lower tensile strength and resilience. Liquid EPDM formulations often get better cross-link density when cured under higher temperature, however, their performance is still generally inferior to that of a vulcanized product. Efforts to both elevate the cure temperature of the liquid EPDM or to find another formulation of room temperature curable, liquid EPDM rubber that yielded a higher cross-link density were not successful.

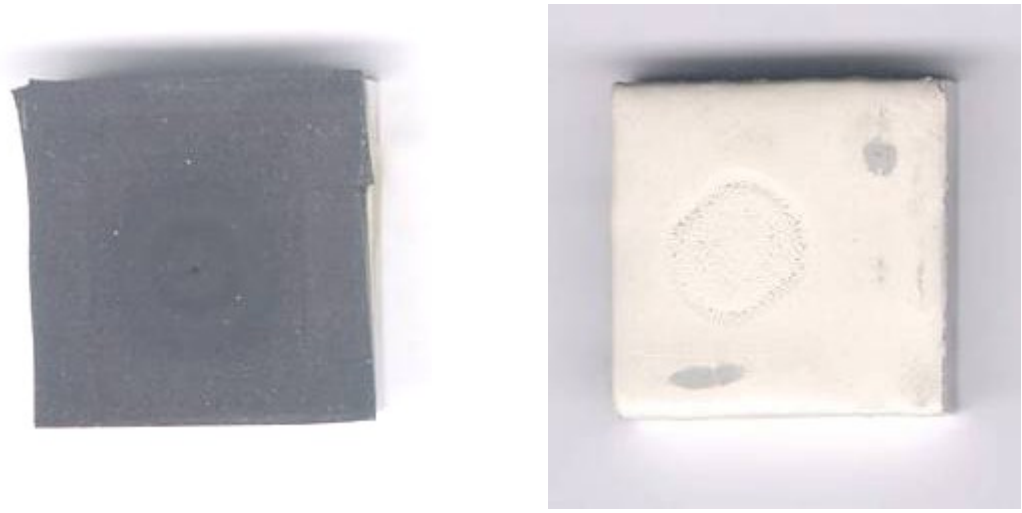

Figure 5.11 – EPDM rubber samples, sheet (left) and liquid (right)

5.3.2 Fluorinated Elastomers

Fluorinated elastomers encompass a class of materials including well-known formulations such as Teflon® and Viton®. Fluorinated elastomers hold a chemical advantage over EPDM formulations by virtue of their higher primary bond cross-link energy [Gouldner, 2002]. The specific formulations tested were all two-part curable liquid formulations from Pelseal® Technologies, LLC. Pelseal® produces a broad range of fluoroelastomer products including adhesives, sealants and coatings. Many of their elastomer products include Viton® as an essential ingredient. By working with one of Pelseal®'s research chemists, we were able to experiment with different formulations in an effort to maximize the cavitation erosion resistance. This work resulted in seven different formulations that were tested. These formulations are listed by Pelseal® descriptors in Table 5.1 along with the results from testing. As noted in the comments section, all the samples showed some kind of cracking or pitting during the testing as

depicted in Figure 5.12. This usually resulted in more severe mass loss as testing continued. None of the samples tested resulted in an erosion rate better than that of 316L stainless.

Table 5.1 - List of custom formulated Pelseal® Technologies samples tested

Pelseal Descriptor	Cure Method	Erosion Rate (μm/hr)	Comments
PLV 2100	Room Temp, Pelseal applied Sample #103	9.49*	cracking, pitting on surface after 350 min
PLV 6032	Elevated Temp, Pelseal applied #106	7.58*	Cracking, pitting after 762 min
PLV 2589	Elevated Temp, Pelseal applied #115,#116,#117	7.24	Cracking, pitting on surface
PLV 6032	Room Temp, Pelseal applied #104	NA	Cracking, pitting on surface after 318 min
PLV 2100	Elevated Temp, Pelseal applied #107, #125	3.1	Pitting on #107
PLV 6096	Elevated Temp, self applied #098	NA	Cracking, pitting on surface after 900 min
PLV 3159	Room Temp, self applied #085	NA	Cracking, pitting on surface after 240 min

* single sample data point

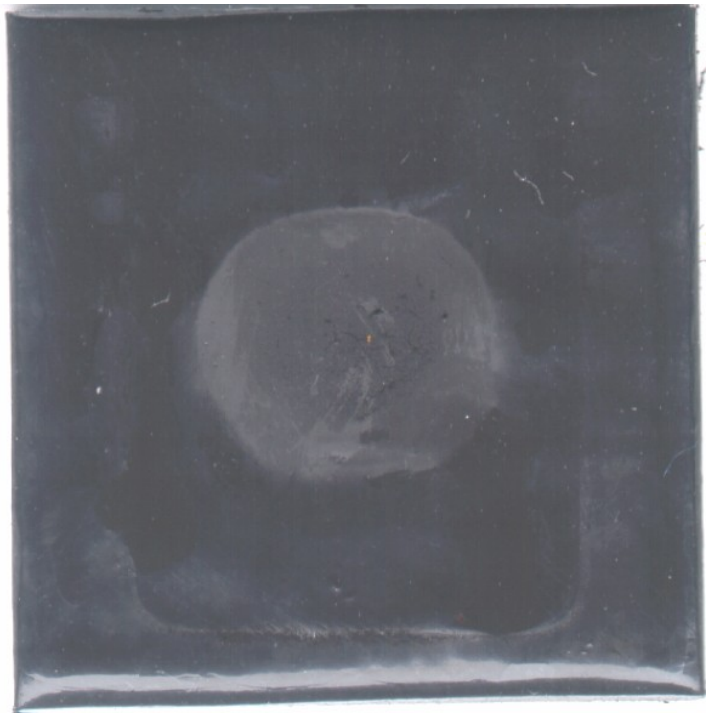

Figure 5.12 – PLV 2100 sample showing typical damage pattern

5.3.3 Polyurethane based Elastomers

Polyurethane based elastomers encompass a wide range of materials including many commercially available protective products. Many of these products are spray-on protective coatings for the lining of truck beds and other uses.

Herculiner® is a one-part paint on polyurethane coating from Old World Industries and is available at many auto parts stores as a truck bed liner product. The material contains large rubber particles intended to be skid resistant. Early screening tests on the material showed that the large rubber granules were early sources of failure and thus the solid particles were strained from the samples using paper paint filters. While most of the granules were filtered, the resulting sample still contained some solid particles.

Otherwise, the samples were prepared per manufacturers specifications on an aluminum substrate. The average thickness was 0.028". The average erosion rate from sample #055 and #057 was 39.2 μm/hr. The failure mechanism in these samples was pitting and loss of the coating as shown in Figure 5.13.

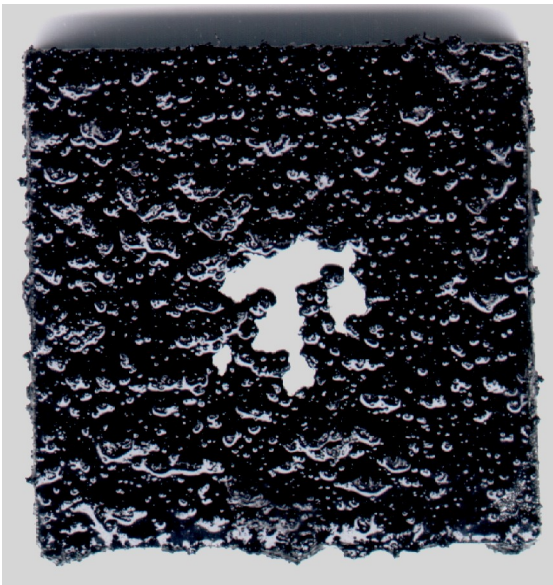

Figure 5.13 - Herculiner® sample #051 showing erosion damage

Rhino Linings® is a commercially available polyurethane truck bed liner from Rhino Linings USA, Inc. It is only available from licensed dealerships and is applied as a two-part spray. The samples were applied at the dealership onto an E-glass substrate. The average thickness was 0.0175". The average erosion rate from samples #137 and #138 was 22.4 μm/hr. The failure mechanism for this material was the formation of a bubble within the coating as shown in Figure 5.14. Dissection of the material revealed that the failure was caused by both delamination of the coating from the substrate and internal shear failure of the material.

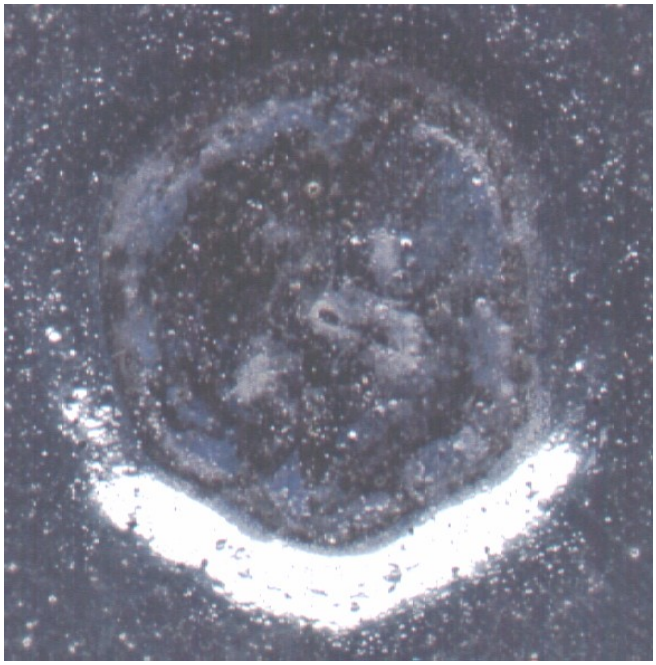

Figure 5.14 – Rhino Linings sample #110 showing typical damage including bubble formation under the horn tip

Arma 952 is a commercially available polyurethane/polyurea blend elastomer from Arma Coatings. The dealer applied the samples onto an aluminum substrate. The average coating thickness was 0.079". In both samples, #089 and #095, severe pitting of the coating prevented a reliable erosion rate reading.

Both Polyshield HT™ and AMP-100™ are polyurea elastomers from Specialty Products, Inc. Only a single sample of each material was tested with erosion rates of 10.4 μm/hr and 5.7 μm/hr respectively. Given its relatively poor performance to the reference material, these coatings were not pursued further.

Aeroshield® is a commercially available polyurethane tape from Scapa North America. It is most commonly used as an erosion protection product for leading edges of aircraft

wings and propellers. It is a thermoplastic product and was much stiffer than other elastomers tested. It came in two-inch wide sheet with its own adhesive backing, which proved to be insufficient during testing on aluminum substrates. Although its resistance to cavitation erosion appeared to be good, actual test results were not recorded because of its hydrophilic nature. Once immersed in water, it was very difficult to properly dry the samples between readings and get accurate results. Given its rigid form and water absorption issues, this material was not pursued further.

5.3.4 Silicone based Elastomers

Silicone based elastomers were a promising category of materials given their high primary bond strength. Two materials were tested in this category. The first was a standard RTV silicone from GE Plastics. Although visual inspection of the erosion resistance was positive, once again, water absorption masked any reasonable data. It was also determined that this material was not abrasive resistant enough for actual in-service application. The second material was Biocoat-A from Analytical Services and Materials, Inc. It is marketed as an erosion and abrasion resistant coating for marine environments. The manufacturer applied the samples to an aluminum substrate at a thickness of 0.010". The average erosion rate of samples #129 and #142 was 2.8 μm/hr. Visible cracking, pitting or other failure signs were not apparent in any of the samples tested as shown in Figure 5.15.

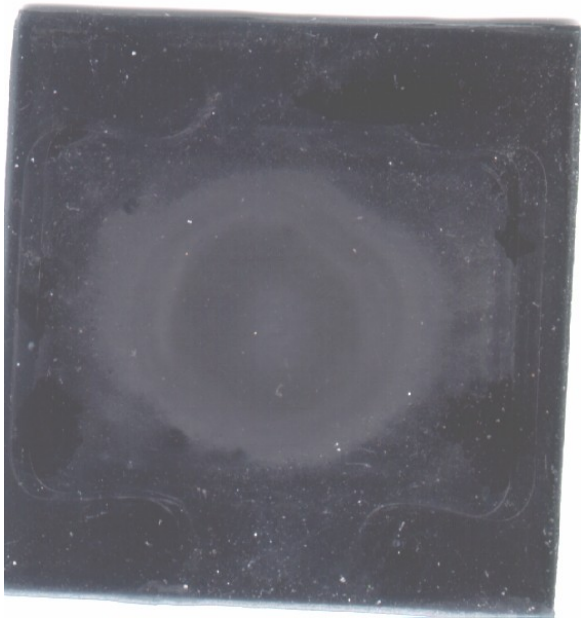

Figure 5.15 – Biocoat-A screening sample #119 after 2,936 minutes of test time. No visible cracking or pitting

5.3.5 Polychloroprene based Elastomer

Cuproprene is manufactured by Dunlaw Engineering Limited and consists of a monolayer of cupro-nickel granules embedded and chemically bonded in a polychloroprene rubber sheet. The material is used primarily on submerged and splash zone structures for its anti-fouling capabilities. The material is available in sheet form and was bonded to an aluminum substrate using a two-part epoxy. The single sample erosion rate of 9.5 μm/hr represents mass loss in the cupro-nickel granules as shown in Figure 5.16. The rubber sheet showed little sign of cavitation damage.

Figure 5.16 – Cuproprene sample showing damage to embedded copper-nickel granules

5.4 Other

Other materials tested include two nylons and a curable ceramic coating. A single sample of Nylon 6, #077, was tested and achieved an erosion rate of 159 μm/hr. A similar nylon material reinforced with random oriented glass fiber, #078, achieved 103 μm/hr. The curable ceramic coating system, CeRam-Kote 54® from Freecom, Inc., was included based on a recommendation from Navatek. The coating consists of an epoxy resin that is filled with ceramic particles. It is used regularly in the marine industry as a hard, abrasion resistant protection mechanism for various components including hulls. The material was applied to an aluminum substrate per manufacturer;s recommencations to a thickness of 0.014". The hard ceramic did not stand up to the cavitation environment

and resulted in an erosion rate of 159 μm/hr from samples #074 and #075. Severe pitting and material loss as shown in Figure 5.17 characterized the ceramic failure.

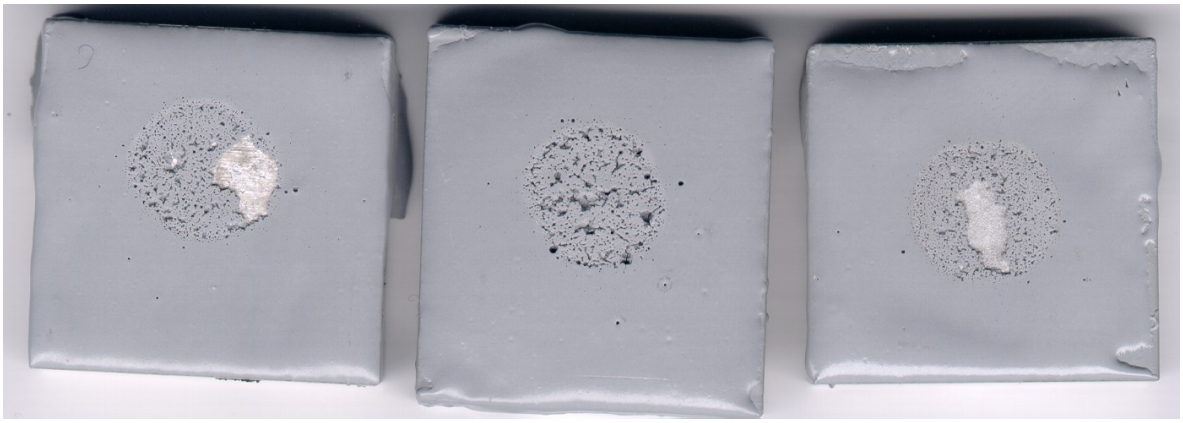

Figure 5.17 – Tested samples of CeRam-Kote 54 on aluminum substrates showing cavitation damage

6. Summary and Recommendations

The goal of the research presented herein was to identify materials and/or methodologies that increased the cavitation erosion resistance of the GRP materials that will be utilized in the MACH program. Each of these material systems was evaluated using a modified ASTM G32 vibratory induced cavitation test method. The modification to the standard methodology involved the physical placement of the specimen to be tested. Instead of mounting the test sample to the vibrating horn, the sample was held stationary at a prescribed distance under the oscillating horn tip. This modification provided increased flexibility in evaluating both cored composites and soft elastomer materials. The modification did however make it difficult to compare the test results with other published data utilizing the standard method. A brief investigation into the causes of this discrepancy did not lead to any conclusive results and thus the reader is cautioned against making direct comparisons of the results reported here with those of other test setups. In order to provide some reference for the results, two common erosion resistant materials, 316L stainless steel and NiAl bronze, were included in the test matrix. These materials provide a direct comparison between the results of this testing and those from other published sources and also provide a baseline erosion resistance to be achieved by the new materials. The method was proven to be repeatable and periodic checks of the apparatus were performed throughout the test series using aluminum as a reference material. The prolonged test times of some of the materials necessitated the addition of a digitally controlled cooling circuit to ensure that the bulk test fluid temperature remained within specified limits.

The materials tested were chosen based on their potential applicability to the objectives of the overall MACH program. Many common metallic and ceramic materials were not tested as part of this study for two reasons. First, the performance of many of these materials is well published in the literature, but more importantly, many of these materials presented either excessive weight or manufacturing concerns that were not in line with the lightweight goals of the MACH program. For these reasons, the testing focused mainly on composite and elastomer materials. Forty different material systems were investigated including specialized composite configurations, polymers, elastomers, and two high strength stainless steels not previously tested in this environment. A total of 149 individual samples were tested for a total cavitation time of 96,509 minutes. The result of each test was a set of data recording mass loss versus time. The calculated parameter of maximum erosion rate was chosen for comparison of all the materials because of its normalization with respect to wide ranges in material density. This parameter is obtained by dividing the mass loss at each time interval by the material density. The physical representation of this parameter is a lineal rate of erosion of the material expressed in micrometers per hour. As with any test method, this parameter only provides a basis for comparison and any candidate material would need to be fully screened with regards to its response under actual cavitation conditions.

Test results of the base GRP material show poor erosion resistance even with a rubber modified resin formulation. The predominant damage mechanism in these tests is pitted matrix erosion followed by fiber damage. An order of magnitude increase in erosion resistance was demonstrated by using a linear PVC core material under a thin composite

skin. The primary damage mechanism in this material system was core deterioration. Although a promising methodology in improving the erosion resistance of composites, manufacturing and repair considerations prevented any further optimization. The most promising test results were seen in some of the elastomer materials. The high strain to failure rates and superior energy absorption characteristics provided for a number of materials that matched or exceeded the reference metal materials. The best of these materials was standard sheet EPDM rubber. With erosion rate results one third that of 316L stainless steel, this material shows good potential if the manufacturing concerns of bonding and working with complex curves can be overcome. Other elastomer families of materials such as silicone and fluoroelastomers also show erosion resistance on par with the reference materials. Advantages of these materials include their sprayable application and relatively easy repair possibilities.

Based on these test results, two materials would be recommended for consideration under the MACH program. If both hull curvatures were slight and the probability of repair was minimal, sheet EPDM rubber would be a good choice of material given its high erosion resistance. In more complicated geometries or in places of intense cavitation attack that would require frequent repair, BIOCOAT-A from Analytical Sciences and Materials would be an adequate choice based on erosion performance. Either of these materials provides a lightweight, erosion resistant coating to any base structural material.

Recommendations for further testing include a more comprehensive review of elastomer materials. Other factors such as material and application cost, marine fouling performance and long-term abrasion resistance should also be more closely investigated.

References

ASTM 1998. "Standard Test Method for Cavitation Erosion Using Vibratory Apparatus: G32-98", *Annual Book of ASTM Standards*, American Society for Testing and Materials: 107-120.

Bhowmick, A.K., Stephens, H.L. 2001. "Handbook of Elastomers", *Marcel Dekker, Inc.*, New York, ISBN: 0-8247-0383-9.

Boy, Jeffrey H., Kumar, A., March, P., Willis, P., Herman, H. 1997. "Cavitation and Erosion Resistant Thermal Spray Coatings", Tennessee Valley Authority.

Djordjevic, Vitomir, Kreiner, Jesa, Stojanovic, Zivojin. 1988. "Cavitation Erosion Esmainiation of Composite Materials", *33rd International SAMPE Symposium*: 1561-1570.

Escaler, X., Avellan, F., Egusquiza, E. 2001. "Cavitation Erosion Prediction from Inferred Forces using Material Resistance Data", *Fourth International Symposium on Cavitation*, Pasadena, CA, June 20-23.

Falcone, A.S., Clark, F., Maloney, P. 1974. "Elastic Pitch Beam Tail Rotor Operational Suitability Investigation", USAAMRDL-TR-74-60, Contract DAAJ02-71-C-0063, U.S. Army Air Mobility Research and Development Laboratory, Fort Eustis, Virginia.

Garcia, R., Hammitt, F.G. 1967. "Cavitation damage and correlation with mechanical and fluid properties", *J. Basic Eng.* D 89 (4): 753-763.

Gouldner, H. 2002. Pro Guard Coatings: Telephone conversations.

Greene, Eric, 1999. "Marine Composites", *Eric Green Associates, Inc.*.

Hammond, Douglas A., Amateau, Maurice F., Queeney, Richard A. 1993. "Cavitation Erosion Performance of Fiber Reinforced Composites", *Journal of Composite Materials*, Vol. 27, No. 16/1993: 1522-1544.

Hattori, Shuji, Ishikura, Ryohei, Zhang, Qingliang 2003. "Construction of Database on Cavitation Erosion and Analyses of Carbon Steel Data", *Fifth International Symposium on Cavitation*, Osaka, Japan, November 1-4.

Heymann, F.J. 1970. "Toward Quantitative Prediction of Liquid Impact Erosion", *ASTM STP* Vol. 474: 212.

Kimmel, B.G. 1974. "Development of Composite Constructions with Improved Rain Erosion Resistance", *Final Report ADA005494*, Hughes Aircraft Company.

Lecoffre, Yves 1995. “Cavitation Erosion, Hydrodynamic Scaling Laws, Practical Method of Long Term Damage Prediction”, *International Symposium on Cavitation*, Deauville, France.

Morch, K.A. 1979. “Dynamics of Cavitation Bubbles and Cavitating Liquids”, *Treatise on Materials Science and Technology* Vol. 16: 309-355.

“Photographs and Movies of Cavitation”, Applied Fluids Engineering Laboratory, Univerity of Tokyo. < http://www.fluidlab.naoe.t.u-tokyo.ac.jp/Research/CavPictures/>

Preece, C.M. 1979. “Cavitation Erosion”, *Treatise on Materials Science and Technology*, 16:296-297.

Richman, R.H., McNaughton, W.P. 1990. “Correlation of cavitation erosion behaviour with mechanical properties of metals”, *Wear 140*: 63-82.

Strong, A. 1989. “Fundamentals of Composites Manufacturing: Materials, Methods and Applications”, *Society of Manufacturing Engineers*, ISBN: 0872633586.

Soyama, H., Kumano, H., Saka, M. 2001. “A new parameter to predict cavitation erosion”, *Fourth International Symposium on Cavitation*, Pasadena, CA, June 20-23.

“The Role of Cavitation in Extracorporeal Shock Wave Lithotripsy”, The Center for Industrial and Medical Ultrasound, Applied Physics Laboratory, University of Washington. <http://cimu.apl.washington.edu/litho.html>

Thiruvengadam, A., Waring, S., 1966. “Mechanical properties of metals and cavitation damage resistance”, *J. Ship Res.*, March: 1-9.

Veerabhadra Rao, P., Martin, C.S., Syamala Rao, B.C., and Lakshaman Rao, N.S., “Estimation of Cavitation Erosion with Incubation Periods and Material Properties”, *Journal of Testing and Evaluation, JTEVA, Vol. 9, No. 3*, May 1981: 189-197.

Weigel, W.D. 1996. “Advanced Rotor Blade Erosion Protection System”, *Final Report USAATCOM TR 95-D-8*, Kaman Aerospace Corporation.

Williams, G.C. 1952. “Rain Erosion of Materials”, *WADC Technical Report 52-105*.

Appendix – Summary of Test Results

Table A.1 – Summary of complete test results

Rank	Material	Metal	Composite	Elastomer	Other	MRE (μm/hr)
36	Black Inflatable Dinghy Antifoul Paint				Black Inflatable Dinghy Antifoul Paint	99999.00
	Red Ultra Antifoul Paint				Red Ultra Antifoul Paint	99999.00
35	PLV 2583, #3			PLV 2583, #3		9999.00
	polyurethane tape				polyurethane tape	9999.00
	RTV silicone			RTV silicone		9999.00
	Arma 952			Arma 952		9999.00
34	Bare Carbon Fiber/8084 resin		Bare Carbon Fiber/8084 resin			1158.86
33	Carbon Fiber/8084 resin		Carbon Fiber/8084 resin			684.07
32	E-glass/411 resin - UMO		E-glass/411 resin - UMO			444.46
31	E-glass/8084 resin - UMO		E-glass/8084 resin - UMO			252.42
30	Nylon 6				Nylon 6	159.03
29	CeRam-Kote				CeRam-Kote	158.52
28	6061-T6 Al	6061-T6 Al				151.76
27	Glass filled Nylon				Glass filled Nylon	103.36
26	Liquid EPDM rubber			Liquid EPDM rubber		80.26
25	Quartz/Core		Quartz/Core			38.19
24	Herculiner			Herculiner		39.16
23	Carbon Fiber/Quartz/8084 resin/Core		Carbon Fiber/Quartz/8084 resin/Core			33.14
22	Rhinoliner			Rhinoliner		22.42
21	Carbon Fiber/Core		Carbon Fiber/Core			20.81
20	Carbon Fiber - FMI		Carbon Fiber - FMI			18.54
19	Ni 200	Ni 200				16.79
18	Polyshield HT			Polyshield HT		10.36
17	PLV 2100, #2			PLV 2100, #2		9.49
16	Cuproprene			Cuproprene		9.48
15	PLV 6032, #4			PLV 6032, #4		7.58
14	PLV 2589, #4			PLV 2589, #4		6.35
13	AMP 100			AMP 100		5.70
12	PLV 6032, #2			PLV 6032, #2		5.15
11	PLV 6096, #3			PLV 6096, #3		3.91
10	PLV 2100, #4			PLV 2100, #4		3.05
9	Biocoat-A			Biocoat-A		2.80

Table A.1 continued

8	316 SS	316 SS				2.28
7	AL-6XN SS	AL-6XN SS				2.10
6	Ni-Al-Bz	Ni-Al-Bz				2.07
5	Zeron 100	Zeron 100				2.00
4	PLV 3159, #1			PLV 3159, #1		1.89
3	Titanium (horn tip)	Titanium (horn tip)				1.80
2	Ferralium	Ferralium				1.63
1	EPDM - sheet			EPDM - sheet		0.72

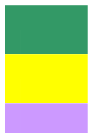

total failure - erosion rate in ficticous water absorption problems

1 sample

Table A.2 – Sample test data sheet

Date:	3/3/2003
Material:	6061-T6 Al
Horn:	101-147-037
Amplitude %:	31
Test # :	096

material density (mg/in^3):	45359
Horn Tip Diameter (in):	0.4134
Horn Tip Area (in^2):	0.1342
Material Thickness (in):	0.25
Volume Under Horn Tip (in^3):	0.0336
Mass Uncertainty (mg):	0.1000
Horn Tip Diameter Uncertainty (in):	0.0197

Notes

clean tip, fresh distilled water, polished with grinding wheel, no visible pitting or scratches

elapsed time (min)	mass (gm)	mass loss (mg)	temp (C)	cumulative mass loss (mg)	mean depth of erosion (μm)	mean depth of erosion uncertainty (μm)
0	10.5406	0	25	0	0	0
10	10.5397	0.9	25	0.9	3.75	0.69
20	10.5368	2.9	25	3.8	15.85	1.62
30	10.5318	5	25	8.8	36.71	3.55
40	10.526	5.8	25	14.6	60.91	5.84
50	10.5193	6.7	25	21.3	88.86	8.49
60	10.5131	6.2	25	27.5	114.73	10.95

maximum rate of erosion (μm/hr)	145.18
y-intercept for maximum erosion rate line	-36
nominal incubation time (min)	14.8

Biography of the Author

Kendrick Light was born in Augusta, Maine on October 31, 1970. He was raised in South China, Maine and graduated from Erskine Academy in 1989. He attended the University of Maine and graduated in 1993 with a Bachelor's degree in Mechanical Engineering. He returned to the University of Maine and entered the Mechanical Engineering graduate program in the fall of 1993. Personal circumstances prevented him from finishing his thesis requirements in the spring of 1996.

Kendrick is currently employed by Applied Thermal Sciences, Inc. in Sanford, Maine and participates in numerous cutting edge research and development projects. Kendrick is a candidate for the Master of Science degree in Mechanical Engineering from The University of Maine in August, 2005.